

2

UNCLASSIFIED
SECURITY CLASSIFICATION OF THIS PAGE

MASTER COPY

FOR REPRODUCTION PURPOSES

REPORT DOCUMENTATION PAGE

| | | | |
|---|---|--|-----------------------|
| 1a. REPORT SECURITY CLASSIFICATION Unclassified | | 1b. RESTRICTIVE MARKINGS DTIC FILE COPY | |
| 2a. SECURITY CLASSIFICATION AUTHORITY | | 3. DISTRIBUTION/AVAILABILITY OF REPORT Approved for public release; distribution unlimited. | |
| AD-A207 387 | | 5. MONITORING ORGANIZATION REPORT NUMBER(S) ARO 24620.3-E6-UIR | |
| 6a. NAME OF PERFORMING ORGANIZATION Massachusetts Institute of Technology, Civil Engineering | 6b. OFFICE SYMBOL (if applicable) CCRE/PACT | 7a. NAME OF MONITORING ORGANIZATION U. S. Army Research Office | |
| 6c. ADDRESS (City, State, and ZIP Code) 77 Massachusetts Avenue, Room 1-175 Cambridge, MA 02139 | | 7b. ADDRESS (City, State, and ZIP Code) P. O. Box 12211 Research Triangle Park, NC 27709-2211 | |
| 8a. NAME OF FUNDING/SPONSORING ORGANIZATION U. S. Army Research Office | 8b. OFFICE SYMBOL (if applicable) | 9. PROCUREMENT INSTRUMENT IDENTIFICATION NUMBER DAAL03-87-K-0005 | |
| 8c. ADDRESS (City, State, and ZIP Code) P. O. Box 12211 Research Triangle Park, NC 27709-2211 | | 10. SOURCE OF FUNDING NUMBERS PROGRAM ELEMENT NO. PROJECT NO. TASK NO. | |
| 11. TITLE (Include Security Classification) Propagation Characteristics of Electromagnetic Waves in Concrete | | | |
| 12. PERSONAL AUTHOR(S) Halabe, Udaya B.; Jaser, Kenneth; Kausel, Eduardo | | | |
| 13a. TYPE OF REPORT Technical | 13b. TIME COVERED FROM 1/88 TO 12/88 | 14. DATE OF REPORT (Year, Month, Day) March 1989 | 15. PAGE COUNT 104 |
| 16. SUPPLEMENTARY NOTATION The view, opinions and/or findings contained in this report are those of the author(s) and should not be construed as an official Department of the Army position, policy, or decision, unless so designated by other documentation. | | | |
| 17. COSATI CODES FIELD GROUP SUB-GROUP | | 18. SUBJECT TERMS (Continue on reverse if necessary and identify by block number) Non Destructive Testing; Wave propagation; Electromagnetic properties of concrete; Concrete permittivity; Ground penetrating radar; infrastructure assessment | |
| 19. ABSTRACT (Continue on reverse if necessary and identify by block number) <p>➤ This research develops models which can predict the velocity and attenuation of electromagnetic waves in concrete as a function of frequency, temperature, moisture content, chloride content and concrete mix constituents. These models have been proposed to predict the electromagnetic properties of concrete by aggregating the electromagnetic properties of its constituents. Water and the dissolved salt are the constituents having the most prominent effect on the dielectric behavior of concrete.</p> | | | |
| 20. DISTRIBUTION/AVAILABILITY OF ABSTRACT <input type="checkbox"/> UNCLASSIFIED/UNLIMITED <input type="checkbox"/> SAME AS RPT. <input type="checkbox"/> DTIC USERS | | 21. ABSTRACT SECURITY CLASSIFICATION Unclassified | |
| 22a. NAME OF RESPONSIBLE INDIVIDUAL | | 22b. TELEPHONE (Include Area Code) | 22c. OFFICE SYMBOL |

DTIC
SELECTED
MAY 01 1989
S E D

19. ABSTRACT (Cont'd)

A comparative study of three existing three-phase mixture models has been carried out. Numerical results have been generated using the most representative "Discrete model". These results have shown that the real part of complex concrete permittivity (and therefore the velocity of electromagnetic waves) is independent of salinity or frequency in the 0.6 to 3.0 GHz frequency range. On the other hand, these results show that the attenuation coefficient and dielectric conductivity vary almost linearly with frequency in this same frequency range. The real part of concrete permittivity and the attenuation coefficient also show a linear dependence with respect to the degree of saturation of water in the concrete mixture. This suggests that future research should focus on approximating the complex models presented in this research by simple equations. (See)

| | |
|--------------------|-------------------------------------|
| Accession For | |
| NTIS GRA&I | <input checked="" type="checkbox"/> |
| DTIC TAB | <input type="checkbox"/> |
| Unannounced | <input type="checkbox"/> |
| Justification | |
| By _____ | |
| Distribution/ | |
| Availability Codes | |
| Dist | Avail and/or Special |
| A-1 | |



**PROPAGATION CHARACTERISTICS OF ELECTROMAGNETIC
WAVES IN CONCRETE**

Technical Report

by

**Udaya B. Halabe (Graduate Research Assistant)
Dr. Kenneth Maser (Research Supervisor)
Prof. Eduardo Kausel (Research Supervisor)**

Period: January, 1988 - December, 1988

U.S. ARMY RESEARCH OFFICE

Grant/Contract No. DAAL 03-87-0005

Massachusetts Institute of Technology
Department of Civil Engineering
Cambridge, MA 02139

Approved for public release;
Distribution unlimited

The views, opinions, and/or findings contained in this report are those of the author and should not be construed as being those of the sponsors.

ABSTRACT

This research develops models which can predict the velocity and attenuation of electromagnetic waves in concrete as a function of frequency, temperature, moisture content, chloride content and concrete mix constituents. These models have been proposed to predict the electromagnetic properties of concrete by aggregating the electromagnetic properties of its constituents. Water and the dissolved salt are the constituents having the most prominent effect on the dielectric behavior of concrete.

A comparative study of three existing three-phase mixture models has been carried out. Numerical results have been generated using the most representative "Discrete model". These results have shown that the real part of complex concrete permittivity (and therefore the velocity of electromagnetic waves) is independent of salinity or frequency in the 0.6 to 3.0 GHz frequency range. On the other hand, these results show that the attenuation coefficient and dielectric conductivity vary almost linearly with frequency in this same frequency range. The real part of concrete permittivity and the attenuation coefficient also show a linear dependence with respect to the degree of saturation of water in the concrete mixture. This suggests that future research should focus on approximating the complex models presented in this research by simple equations.

TABLE OF CONTENTS

| | <u>Page No.</u> |
|--|-----------------|
| TITLE PAGE | i |
| ABSTRACT | ii |
| TABLE OF CONTENTS | iii |
| LIST OF FIGURES | iv |
| LIST OF TABLES | v |
| NOTATION | vi |
| CHAPTER 1 INTRODUCTION | 1 |
| CHAPTER 2 MODELLING OF DIELECTRIC PROPERTIES | 5 |
| 2.1 Introduction | 5 |
| 2.2 Models for Dielectric Properties of Saline Water | 7 |
| 2.3 Models for Dielectric Properties of Concrete | 20 |
| CHAPTER 3 NUMERICAL STUDIES | 32 |
| 3.1 Introduction | 32 |
| 3.2 Data Used for Numerical Study | 32 |
| 3.3 Numerical Results | 37 |
| CHAPTER 4 CONCLUSIONS | 60 |
| APPENDIX I REFERENCES | 64 |
| APPENDIX II CONVERSION OF ELECTRICAL UNITS TO "SI" UNITS | 66 |
| APPENDIX III NUMERICAL PROCEDURE FOR OBTAINING ROOTS OF COMPLEX EQUATIONS | 67 |
| (a) Obtaining Real and Complex Roots | 67 |
| (b) Computer Programs and Subroutines (FORTRAN-77) | 67 |

LIST OF FIGURES

| <u>Figure No.</u> | <u>Title</u> | <u>Page No.</u> |
|-------------------|--|-----------------|
| 1 | (a) Real and (b) Imaginary, Parts of the Complex Dielectric Constant of Water | 14 |
| 2 | (a) Static Dielectric Constant (b) Relaxation time, of Aqueous NaCl Solutions | 18 |
| 3 | Comparison of Resistivities of Pore and Bulk Water | 18 |
| 4 | Permittivity of Concrete as a Function of Frequency (Discrete Model) | 51 |
| 5 | Loss Factor of Concrete as a Function of Frequency (Discrete Model) | 52 |
| 6 | Attenuation Coefficient of Concrete as a Function of Frequency (Discrete Model) | 53 |
| 7 | Dielectric Conductivity of Concrete (Discrete Model) | 54 |
| 8 | Permittivity of Concrete as a Function of Degree of Saturation (Discrete Model) | 55 |
| 9 | Attenuation Coefficient of Concrete as a Function of Degree of Saturation (Discrete Model) | 56 |

LIST OF TABLES

| <u>Table No.</u> | <u>Title</u> | <u>Page No.</u> |
|------------------|---|-----------------|
| 1 | Comparison of Complex CRIM vs Real CRIM | 38 |
| 2 | Comparison of the Three Mixture Models | 40 |
| 3 | Effect of Slight Change in Concrete Composition on Results Predicted by Discrete Model | 49 |
| 4 | Effect of Temperature Change on Dielectric Properties of Concrete | 58 |

NOTATION

(a) English Letters

| | |
|-----------------------------|---|
| A | a constant in equation relating salinity to normality |
| A_i | desired final proportion of inclusion in i^{th} step (Discrete Model) |
| a, b, a_1 , b_1 , c_1 | parameters which are functions of water temperature and salinity |
| a' , b' , c' | parameters for Continuous model |
| c | velocity of propagation of electromagnetic wave in a medium (m/sec) |
| c_0 | velocity of electromagnetic waves in vacuum = 3×10^8 m/sec |
| d_p | penetration depth (m^{-1}) |
| \bar{E} | electric field vector (volts/m) |
| E_0 | initial wave amplitude (i.e., amplitude of electric field) in volts/m |
| e | constant = 2.718 |
| f | electromagnetic wave frequency (Hz) |
| f_r | relaxation frequency of saline water (Hz) |
| \bar{H} | magnetic field vector (amperes/m) |
| i | imaginary number ($\sqrt{-1}$) |
| k | complex wavenumber in the medium (m^{-1}) |

| | |
|------------|--|
| k_R | real part of complex wave number (m^{-1}) |
| k_I | imaginary part of complex wave number = attenuation coefficient (m^{-1}) |
| k' | number of inclusions at each step (Discrete model) |
| N_{sw} | normality of saline water |
| m', n' | parameters for Continuous model |
| m'', n'' | exponents in the Archie's Law expression for dc conductivity |
| P_i | volume fraction of the inclusion in i^{th} step (Discrete model) |
| R_{12} | reflection coefficient for wave amplitude for wave propagating from medium 1 into medium 2 |
| S | degree of saturation in concrete = (volume of water)/ (volume of voids) |
| S_{sw} | salinity of water in parts per thousand (ppt) by weight |
| T | temperature ($^{\circ}C$) |
| T_{12} | transmission coefficient for wave amplitude for wave propagating from medium 1 into medium 2 |
| t | time (sec) |
| v_a | volume fraction of air in the concrete mixture |
| v_i | volume fraction of i^{th} constituent of concrete |
| v_m | volume fraction of solid particles in the concrete mixture |
| v_w | volume fraction of water in the concrete mixture |

| | |
|-----------|--|
| \hat{x} | unit vector along x-direction (i.e., direction of wave propagation) |
| \hat{y} | unit vector along y-direction (i.e., perpendicular to the direction of wave propagation) |
| x, y, z | co-ordinate axes |
| Z | intrinsic wave impedance of the medium (ohm) |

(b) Greek Letters

| | |
|-------------|--|
| Π | constant = 3.142 |
| ω | angular frequency (rad/sec) |
| λ | wavelength of propagating electromagnetic wave (m) |
| ϕ | parameter which depends on water temperature and salinity |
| θ | phase shift associated with intrinsic impedance of a medium |
| ϕ | porosity of concrete |
| δ | loss angle in concrete |
| δ_w | loss angle in water |
| τ_{sw} | relaxation time of saline water (sec) |
| Δ | parameter equal to $(25-T) \text{ }^\circ\text{C}$ |
| ∇^2 | Laplacian operator = $\frac{\partial^2}{\partial x^2} + \frac{\partial^2}{\partial y^2} + \frac{\partial^2}{\partial z^2}$ |
| η_t | refractive index for a medium |

| | |
|-----------------------|---|
| μ_0 | permeability of free space = $4\pi \times 10^{-7}$ henry/m |
| μ_t | permeability of a medium = μ_0 for most dielectric materials |
| ϵ | relative dielectric permittivity of concrete (dimensionless) |
| ϵ' | real part of ϵ (dimensionless) |
| ϵ'' | imaginary part of ϵ (dimensionless) |
| ϵ_a | relative dielectric permittivity of air $\cong 1.0$ |
| ϵ_i | dielectric permittivity of i^{th} constituent of concrete |
| ϵ_m | relative dielectric permittivity of concrete solids $\cong 5.0$ |
| ϵ_0 | dielectric permittivity of free space = 8.854×10^{-12} farad/m |
| ϵ_{sw} | complex relative dielectric constant of saline water (dimensionless) |
| ϵ'_{sw} | real part of ϵ_{sw} (dimensionless) |
| ϵ''_{sw} | imaginary part of ϵ_{sw} (dimensionless) |
| ϵ_{sw0} | static dielectric constant of saline water (dimensionless) |
| $\epsilon_{sw\infty}$ | very high frequency (or optical) limit of ϵ_{sw} (dimensionless) |
| σ | dielectric conductivity of concrete (mho/m) |
| σ_c | complex conductivity of concrete (mho/m) |

- σ_i ionic (i.e., ohmic or dc) conductivity of aqueous saline solution (mho/m)
- σ_j complex conductivity of j^{th} inclusion in the Discrete model (mho/m)
- σ_n complex conductivity of the mixture upto n^{th} step in the Discrete model (mho/m)
- σ_{n-1} complex conductivity of the mixture upto (n-1)th step in the Discrete model (mho/m)
- σ_o dc conductivity of the concrete mixture (mho/m)
- σ_w dielectric conductivity of water (mho/m)

CHAPTER 1

INTRODUCTION

The objective of this project is to develop an electromagnetic wave propagation technique for the assessment of the subsurface condition of reinforced concrete structures using ground penetrating radars. Concrete bridge decks have been studied in particular because they have been the focus of other ongoing research at MIT which have provided actual field data. In addition, concrete bridge decks incorporate many characteristic features of other reinforced concrete structures, and thus the specific results obtained from this study can be generalized without much difficulty to other related applications.

Ground penetrating radar is the electromagnetic analog of sonar and ultrasonic pulse-echo methods. The radar antenna can be either in contact with the bridge deck slab or 10 to 30 centimeters above it. A short (0.5 to 1.5 ns.) pulse of electromagnetic energy is transmitted into the slab, which then gets reflected from objects or interfaces which represent discontinuities in electrical properties (Maser, 1989). In a bridge deck, such discontinuities include the asphalt/concrete interface, top and bottom rebar grid, the bottom of the slab, and abrupt variations in concrete properties. The reflected echo signal is then picked up by a receiving antenna, which is usually same as - or located adjacent to - the transmitting antenna (Maser,

1989). Another typical characteristic of commercial antennas is that they are linearly polarized. This means that they will tend to show a much stronger response to rebars, cylinders, or other subsurface anomalies oriented parallel to the polarization direction of the electric field. The time history of these reflected signals is referred to as the "waveform".

The strength of the peaks in this waveform (which correspond to the subsurface interfaces and anomalies) depend on the reflection, transmission and attenuation characteristics of the medium. The reflection and transmission coefficient at an interface depends on the velocity of the layers on either side, which in turn depends on their dielectric properties. The relative position of the peaks in the waveform also depends on these velocities. Thus, velocity and attenuation of electromagnetic waves in the medium are the two main parameters affecting the output waveform, and these parameters are related to the complex dielectric permittivities of the various underlying layers.

During the first year of this project (January to December, 1987) the focus of research was on modelling the reflection of electromagnetic waves by metallic cylindrical objects buried in concrete and on the synthesis of radar waveforms from concrete bridge decks (Maser and Halabe,1988). Experiments were carried out to observe reflections from rebars and cylinders suspended in air and buried in sand. These reflections were then modelled using a Scattering Attenuation Function (SAF) which was derived from principles in geometric optics. This model for rebars was then

incorporated in a computer program for waveform synthesis. The dielectric properties of concrete were modelled using a simple three-phase mixture formula and radar waveforms were synthesized for normal concrete, low-moisture deteriorated concrete and for high-moisture deteriorated concrete. A comparison of these synthesized waveforms with radar waveforms obtained from actual bridge decks showed that the field waveforms incurred considerably higher attenuation than that predicted by the synthesis model. Thus, there was a need for improved understanding of the velocity and attenuation characteristics of electromagnetic waves in reinforced concrete.

The objective in this year's research has been to characterize the velocity and attenuation of electromagnetic waves in reinforced concrete as a function of frequency, temperature, moisture content, chloride content and concrete mix constituents. This objective has been pursued by adaptation of theoretical models which have been developed and verified for partially saturated rocks. In these models, the electromagnetic properties of the medium has been modelled by aggregating the properties of its most significant constituents. The research described herein has adapted these aggregating techniques to reinforced concrete, whose significant constituents are coarse aggregate, fine aggregate, cement paste, air, water, salt and steel rods. Although the volumetric content of water in a concrete mixture is usually small compared to the volume of aggregates, it has the most significant contribution towards the dielectric permittivity of the overall mixture because of its high complex dielectric

permittivity. This electromagnetic property of water is, in turn, highly sensitive to the amount of dissolved salts. Hence, emphasis in this study has been placed on modelling of dielectric properties of saline water.

The following chapters will describe the various models that have been considered, and the numerical results obtained.

CHAPTER 2

MODELLING OF DIELECTRIC PROPERTIES

2.1 Introduction

A dielectric material is a material which conducts electromagnetic waves, and is commonly referred to as an 'insulator'. The transition from insulator (which is characterized by low electric conductivity) to conductor (which has high conductivity) is a gradual one without any clear cut-off point, and many existing materials exhibit both properties. If the conductivity of a material is high, it attenuates electromagnetic waves to a larger extent, thus resulting in a lower penetration depth. The two significant properties of a dielectric material are the real and imaginary parts of its complex dielectric permittivity. The real part is associated with the phase velocity and the imaginary part signifies the conductivity or attenuation of electromagnetic waves in the medium. The dielectric permittivity is often referred to as the dielectric 'constant'. This term is a misleading one, since this property of a dielectric material varies with several factors. Bell, et. al. (1963) have provided some insight into these variations through underlying molecular and atomic mechanisms associated with dielectric constant and conductivity of such materials.

A dielectric material increases the storage capacity of a capacitor by neutralizing charges at the electrode surfaces. This

neutralization can be imagined to be the result of the orientation or creation of dipoles opposing the applied field. Such a polarization is proportional to the polarizability of the dielectric material; that is, the ease with which it can be polarized. Polarizability is defined as the average induced polarization per unit field strength. The greater the polarizability of a material, the greater will be its dielectric constant.

There are four recognized mechanisms of polarization: (a) electronic, (b) atomic, (c) orientation, and (d) space charge or interfacial mechanism. The first three polarization mechanisms are forms of the dipole polarization previously mentioned. They result from the presence of permanent dipoles or from dipoles induced by external fields. The fourth type - space charge polarization - results from charge carriers that are usually present and more or less free to move through the dielectric. When such carriers are impeded in their movement and become trapped in the material or at interfaces, space charge concentrations result in a field distortion that increases the capacitance.

The above discussions indicate that the dielectric constant of a material is not such a constant, but is a function of the polarizability which is in turn a function of frequency, temperature, local fields, applied field strength, availability and freedom of charge carriers within the dielectric, and local field distortions.

The dielectric conductivity (defined later in Eq. 7) is also affected by the same factors. This is because the dielectric

conductivity is a function not only of ohmic conductivity but also of the power consumed in polarizing the material.

In addition to the 'intrinsic loss' caused by the conduction process, there could also be 'scattering loss' due to the presence of inhomogeneities within the medium. Since the aggregate particle size is much smaller than the electromagnetic wavelength considered here ($\lambda \cong 10$ cm in concrete), the inhomogeneities in concrete are not likely to cause significant scattering losses. However, this is not true for inhomogeneities with large dimension (like delaminations) or with large conductivity (like rebars). These inhomogeneities will be modelled separately and their effect will be taken into account for the purpose of waveform synthesis.

2.2 Models for Dielectric Properties of Saline Water

Moisture and chloride are the two constituents which have the most prominent effect on the dielectric properties of concrete. Although the volumetric content of water in a concrete mixture is small, it has a very important bearing on the velocity and attenuation of electromagnetic waves in concrete because of its high complex dielectric permittivity. Repeated application of de-icing salts over concrete bridge decks in winter months along with the cracking of the concrete due to freeze-thaw cycles cause the salt to infiltrate into the bridge decks. This salt is commonly referred to as free chlorides because it can readily go into solution (as opposed to chloride components which are chemically bound in the cement

paste). Only the chlorides which are actually present in solution form at any given time affects the dielectric properties of water and of the concrete mixture as a whole. Presence of dissolved chlorides reduces the real part of the complex dielectric permittivity of water (which affects the radar velocity), and greatly increases the imaginary part (which affects the attenuation of radar waves). The latter effect is due to the increase in ohmic conductivity of water. In addition, temperature of water affects its conductivity, and is thus another factor affecting its dielectric properties. A model for predicting these dielectric properties of water is presented in the next paragraph.

Various researchers (e.g., Dorsey, 1940; Saxton, 1952b; Stogryn, 1971) have formulated empirical models to fit the observed experimental results for dielectric properties of aqueous sodium chloride (NaCl) solutions. Some of the predicted values have been tabulated by Dorsey (1940) and Saxton (1952b). Earlier models presented by Dorsey (1940) prescribe different equations for different temperatures, and thus are difficult to use. The model by Saxton (1952b) is also difficult to use because of its complicated form. Recent work in this area have removed these problems and have improved the accuracy of prediction (Ulaby et al, 1986). Ulaby et al (1986) have presented models developed recently which are discussed below. These are empirical models obtained by a non-linear regression analysis to fit the experimental data compiled by several researchers.

A model for pure and saline water was developed by Stogryn (1971) and later modified by Klein and Swift (1977). Since tap water or water in the pores of concrete is never pure, the pure water model is not of much interest here. The salinity (S_{sw}) of a salt solution is defined as the total mass of solid salt in grams dissolved in one kilogram of the aqueous solution. Thus, S_{sw} is expressed in parts per thousand (ppt) by weight. The normality of saline water (N_{sw}) is related to its salinity by the following expression (Klein, 1977):

$$N_{sw} = A S_{sw} [1.707 \times 10^{-2} + 1.205 \times 10^{-5} S_{sw} + 4.058 \times 10^{-9} S_{sw}^2] \quad (1)$$

where $A=1$ for sodium chloride (NaCl) solution, and $A=0.9141$ for sea water, which includes other salts as well. The above equation is valid for $S_{sw} < 260$ ppt.

The frequency dependence of the complex dielectric constant (ϵ_{sw}) of saline water is given by the well-known Debye equation (Ulaby, 1986):

$$\epsilon_{sw} = \epsilon_{sw\infty} + \frac{\epsilon_{sw0} - \epsilon_{sw\infty}}{1 - i 2\pi f \tau_{sw}} + \frac{i \sigma_i}{2\pi \epsilon_0 f} \quad (2)$$

where,

ϵ_{sw0} = static dielectric constant of saline water (dimensionless)

$\epsilon_{sw\infty}$ = very high frequency (or optical) limit of ϵ_{sw}
(dimensionless)

τ_{sw} = relaxation time of saline water (seconds)

- f = electromagnetic frequency (Hz)
 ϵ_0 = dielectric permittivity of free space = 8.854×10^{-12}
farad/m
 σ_i = ionic (i.e., ohmic or dc) conductivity of the aqueous
saline solution (mho/m)

Upon rationalizing Eq. (2), ϵ_{sw} can be expressed in terms of real and imaginary parts as:

$$\epsilon_{sw} = \epsilon'_{sw} + i \epsilon''_{sw} \quad (3)$$

where the real and imaginary parts are given by:

$$\epsilon'_{sw} = \epsilon_{sw\infty} + \frac{\epsilon_{sw0} - \epsilon_{sw\infty}}{1 + (2\pi f \tau_{sw})^2} \quad (4)$$

and

$$\epsilon''_{sw} = \frac{2\pi f \tau_{sw} (\epsilon_{sw0} - \epsilon_{sw\infty})}{1 + (2\pi f \tau_{sw})^2} + \frac{\sigma_i}{2\pi \epsilon_0 f} \quad (5)$$

The imaginary part (ϵ''_{sw}) is also termed as the 'loss factor'. For pure water σ_i is zero and hence the second term in Eq. (5) vanishes. The loss tangent (also called 'dissipation factor') in water is defined as:

$$\tan \delta_w = \frac{\epsilon''_{sw}}{\epsilon'_{sw}} \quad (6)$$

The dielectric conductivity of water is defined as:

$$\sigma_w = \omega \epsilon''_{sw} \epsilon_0 \quad (7)$$

where ω is the angular frequency ($=2\pi f$). This conductivity is a frequency dependent quantity which can be caused by the

movement of charged bodies such as ions, the orientation of dipoles, or any other process of energy dissipation (Bell et al, 1963). It can be seen from Eqs. (5) and (7) that in the d.c. limit ($\omega \rightarrow 0$) the dielectric conductivity (σ_w) is nothing but the ionic conductivity (σ_i) of water.

According to Stogryn (1971) there is no evidence to indicate that $\epsilon_{sw\infty}$ depends on salinity, and a value of $\epsilon_{sw\infty} = 4.9$ provides a good fit to the available data. The dependence of ϵ_{sw0} on S_{sw} (ppt) and temperature, T ($^{\circ}C$) can be obtained using the following empirical expressions developed by Klein and Swift (1977):

$$\epsilon_{sw0}(T, S_{sw}) = \epsilon_{sw0}(T, 0) \cdot a(T, S_{sw}) \quad (8)$$

where,

$$\begin{aligned} \epsilon_{sw0}(T, 0) = & 87.134 - 1.949 \times 10^{-1} T - 1.276 \times 10^{-2} T^2 \\ & + 2.491 \times 10^{-4} T^3 \end{aligned} \quad (9)$$

$$\begin{aligned} a(T, S_{sw}) = & 1.0 + 1.613 \times 10^{-5} T S_{sw} - 3.656 \times 10^{-3} S_{sw} \\ & + 3.210 \times 10^{-5} S_{sw}^2 - 4.232 \times 10^{-7} S_{sw}^3 \end{aligned} \quad (10)$$

The above equations are valid for salinities in the range $4 < S_{sw} < 35$ ppt. The form used in Eq. (8) may also be used to define the relaxation time,

$$\tau_{sw}(T, S_{sw}) = \tau_{sw}(T, 0) \cdot b(T, S_{sw}) \quad (11)$$

Here $\tau_{sw}(T,0)$ is the relaxation time for pure water and can be obtained using the following expression presented by Stogryn (1971):

$$2\pi \tau_{sw}(T,0) = 1.1109 \times 10^{-10} - 3.824 \times 10^{-12}T + 6.938 \times 10^{-14}T^2 - 5.096 \times 10^{-16} T^3 \quad (12)$$

A related term used in the literature is the relaxation frequency (f_r), where,

$$f_r = (2\pi \tau_{sw})^{-1} \quad (13)$$

It can be seen from Eq. (5) that the first component of ϵ''_{sw} has its maximum value at $f = f_r$. The expression for $b(T, S_{sw})$ was first presented by Stogryn (1971) and later modified by Klein and Swift (1977) through the use of Eq. (1) to yield:

$$b(T, S_{sw}) = 1.0 + 2.282 \times 10^{-5} T S_{sw} - 7.638 \times 10^{-4} S_{sw} - 7.760 \times 10^{-6} S_{sw}^2 + 1.105 \times 10^{-8} S_{sw}^3 \quad (14)$$

This expression is based on data for $0 \leq T \leq 40^\circ\text{C}$ and $0 \leq N_{sw} \leq 3$ (or approximately, $0 \leq S_{sw} \leq 157$ ppt for an NaCl solution).

The only parameter that now remains is the ionic conductivity, σ_i . For sea water, σ_i was derived by Weyl (see Stogryn, 1971) and later modified by Stogryn (1971) to the following form:

$$\sigma_i(T, S_{sw}) = \sigma_i(25, S_{sw}) e^{-\phi} \quad (15)$$

where $\sigma_i(25, S_{sw})$ is the ionic (i.e., ohmic or dc) conductivity of saline water at 25 °C and is given by:

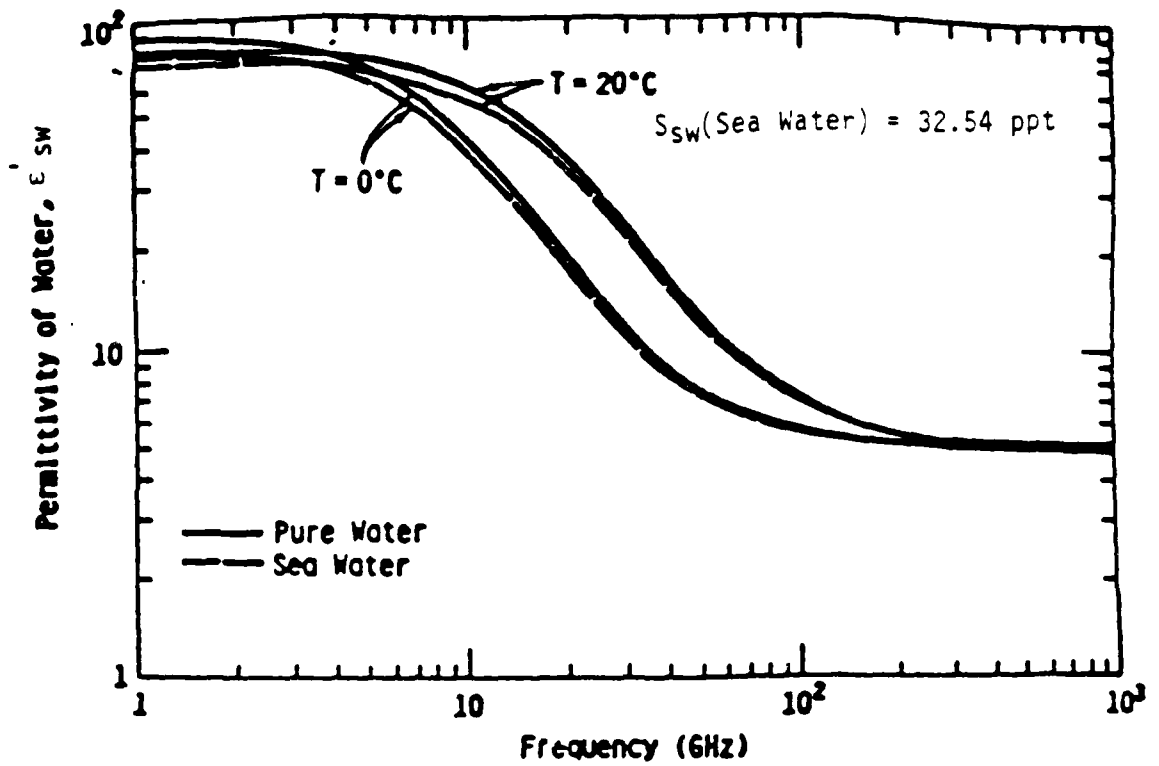
$$\begin{aligned} \sigma_i(25, S_{sw}) = S_{sw} [0.18252 - 1.4619 \times 10^{-3} S_{sw} + 2.093 \times 10^{-5} S_{sw}^2 \\ - 1.282 \times 10^{-7} S_{sw}^3] \end{aligned} \quad (16)$$

The function ϕ in Eq. (15) depends on S_{sw} and $\Delta = 25 - T$,

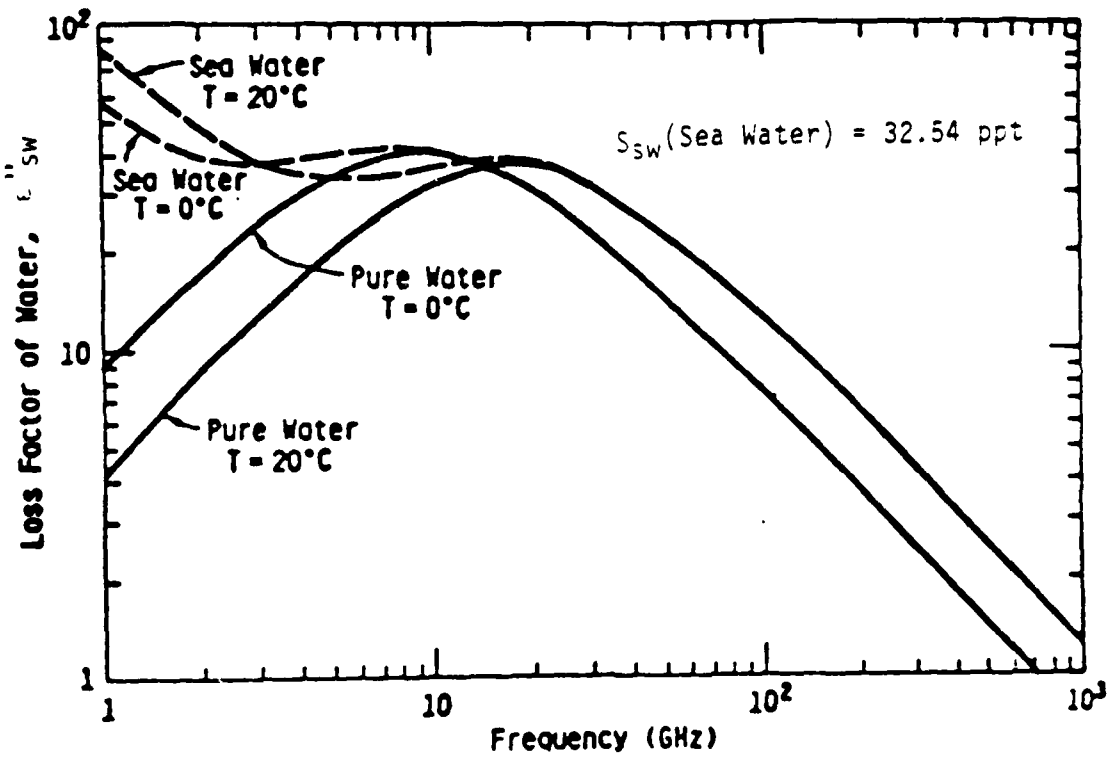
$$\begin{aligned} \phi = \Delta [2.033 \times 10^{-2} + 1.266 \times 10^{-4} \Delta + 2.464 \times 10^{-6} \Delta^2 \\ - S_{sw}(1.849 \times 10^{-5} - 2.551 \times 10^{-7} \Delta + 2.551 \times 10^{-8} \Delta^2)] \end{aligned} \quad (17)$$

The above expressions are valid in the range $0 \leq S_{sw} \leq 40$ ppt. Different expressions presented in this section are valid over different salinity ranges. The combination of these equations is valid in the range $4 \leq S_{sw} \leq 35$ ppt and $0 \leq T \leq 40$ °C. The above model can also be used for pure water ($S_{sw} = 0$) with one small variation. For pure water, Eq. (9) for ϵ_{sw0} will have to be replaced by the following expression given by Klein and Swift (1977).

$$\begin{aligned} \epsilon_{sw0}(\text{pure water}) = 88.045 - 0.4147T + 6.295 \times 10^{-4}T^2 \\ + 1.075 \times 10^{-5}T^3 \end{aligned} \quad (18)$$



(a)



(b)

Figure 1 (a) Real and (b) Imaginary, Parts of the Complex Dielectric Constant of Water (from Ulaby et al, 1986)

The spectral variations and dielectric relaxation phenomena for ϵ'_{sw} and ϵ''_{sw} are shown in Figure 1 for pure water and saline water with $S_{sw} = 32.54$ ppt, which is an average value for sea water (Ulaby, 1986). The relaxation frequency (f_0) of pure water is nearly 9 GHz at 0°C and 17 GHz at 20°C . It can be seen from Figure 1 that presence of dissolved chlorides has a very prominent effect on the loss factor of water, particularly in the 'radar' range (0.1 to 10.0 GHz).

The above model ($S_{sw} < 35$ ppt) is adequate for concrete exposed to a marine environment. However, a significantly higher salinity (of the order of 140 ppt) has been reported for concrete bridge decks (see computations in the chapter on 'numerical studies'). The chloride content at saturation is 357 ppt for cold water and 391.2 ppt for hot water (Weast, 1986). Water with such high salinity is commonly referred to as 'brine'. A model for dielectric permittivity of brine was developed by Stogryn (1971) and is presented below. This model has been developed to fit the observed experimental data in the range $0 \leq N_{sw} \leq 3$ (i.e., $0 \leq S_{sw} \leq 157$ ppt for NaCl solutions) and $0 \leq T \leq 40^\circ\text{C}$. However, for $S_{sw} \leq 35$ ppt, the equations presented earlier in this section give more accurate predictions (Klein, 1977).

In terms of Stogryn's (1971) formulation for brine:

$$\epsilon_{sw0}(T, N_{sw}) = \epsilon_{sw0}(T, 0) \cdot a_1(N_{sw}) \quad (19)$$

$$\tau_{sw}(T, N_{sw}) = \tau_{sw}(T, 0) \cdot b_1(T, N_{sw}) \quad (20)$$

$$\sigma_i (T, N_{sw}) = \sigma_i (25, N_{sw}) \cdot c_1 (\Delta, N_{sw}) \quad (21)$$

The above functions are given by the following expressions:

$$\epsilon_{swo} (T,0) = \epsilon_{swo} \text{ (pure water) given by Eq. (18).}$$

$$\begin{aligned} a_1(N_{sw}) = & 1.0 - 0.255 N_{sw} + 5.15 \times 10^{-2} N_{sw}^2 \\ & - 6.89 \times 10^{-3} N_{sw}^3 \end{aligned} \quad (22)$$

$\tau_{sw} (T,0)$ is defined by Eq. (12).

$$\begin{aligned} b_1 (T, N_{sw}) = & 1.0 + 0.146 \times 10^{-2} T N_{sw} - 4.896 \times 10^{-2} N_{sw} \\ & - 2.97 \times 10^{-2} N_{sw}^2 + 5.64 \times 10^{-3} N_{sw}^3 \end{aligned} \quad (23)$$

Combining Eqs. (1) and (16), with $A=1$ for NaCl solution, we obtain:

$$\begin{aligned} \sigma_i (25, N_{sw}) = & N_{sw} (10.39 - 2.378 N_{sw} + 0.683 N_{sw}^2 - 0.135 N_{sw}^3 \\ & + 1.01 \times 10^{-2} N_{sw}^4) \end{aligned} \quad (24)$$

The last parameter c_1 depends on N_{sw} and $\Delta = 25 - T$,

$$\begin{aligned} c_1 (\Delta, N_{sw}) = & 1.0 - 1.96 \times 10^{-2} \Delta + 8.08 \times 10^{-5} \Delta^2 \\ & - N_{sw} \Delta [3.02 \times 10^{-5} + 3.92 \times 10^{-5} \Delta \\ & + N_{sw} (1.72 \times 10^{-5} - 6.58 \times 10^{-6} \Delta)] \end{aligned} \quad (25)$$

It has been observed by Saxton (1952a) that the dielectric behavior of liquid water is continuous down to -8°C . Hence the above model is

expected to be equally valid for liquid water at temperatures below 0°C (Ulaby, 1986).

Figure 2 gives the static dielectric constant (ϵ_{sw0}) and the relaxation time (τ_{sw}) of aqueous sodium chloride (NaCl) solutions as a function of normality and temperature as computed from Eqs. (19) to (21). It is interesting to note in Figure 2(a) that ϵ_{sw0} for water can drop down to even 40 at high salinity and temperature. It can be noted from Eq. (5) that for small frequencies (in the MHz range) the conductivity term (i.e., the second term) dominates the dielectric relaxation term (i.e., the first term), but at higher frequencies (GHz range) the relaxation effect could be significant.

The models described earlier in this section are applicable to water in bulk. However, some researchers have pointed out that the dielectric behavior of adsorbed water (i.e., water in contact with the surface of pores of rocks and soils) is slightly different from that of bulk water because the relaxation frequency for adsorbed water is a bit lower (Hoekstra, 1974) and the ionic conductivity is altered (Keller, 1966). When an electrolyte is in contact with a surface, several layers of water molecules will become adsorbed to the surface. The conductivity of water in this oriented adsorbed phase is higher than the conductivity of free water, and so contributes to the overall conductivity of a rock (Keller, 1966). On the other hand, the increased pressure in the adsorbed layers increases the viscosity of the water and decreases the mobility of ions. If many ions are adsorbed, the water conductivity may be significantly reduced

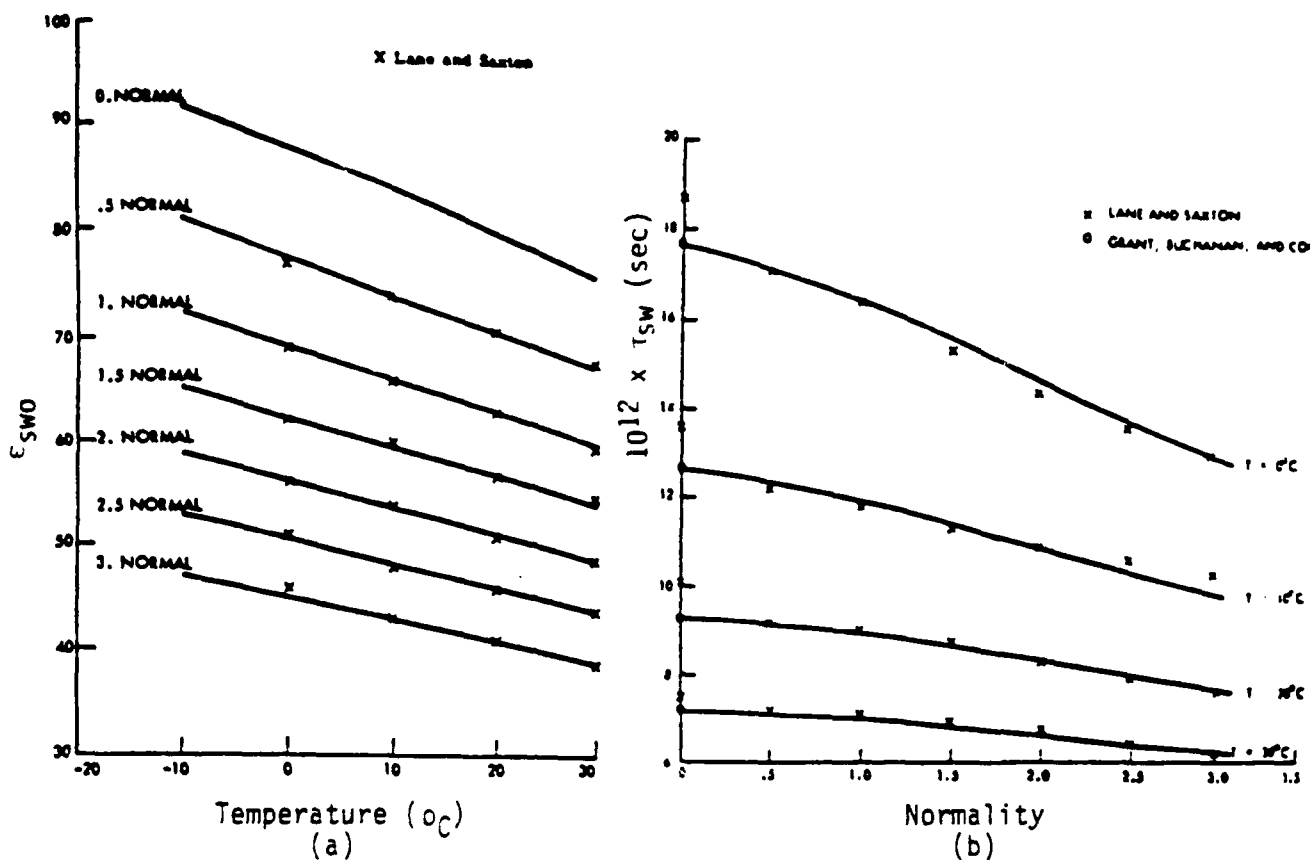


Figure 2. (a) Static Dielectric Constant (b) Relaxation Time, of Aqueous NaCl Solutions (from Stogryn, 1971)

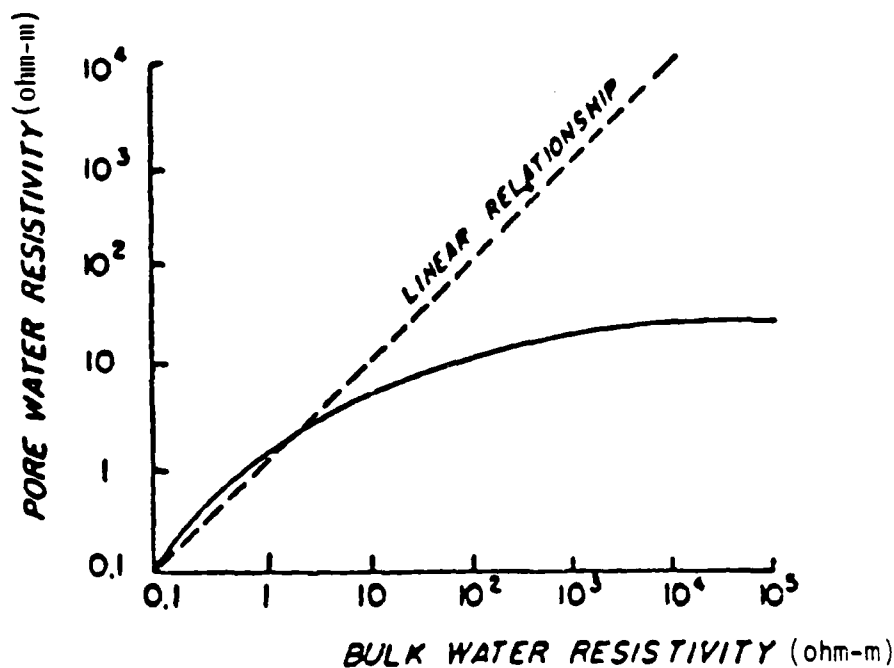


Figure 3. Comparison of Resistivities of Pore and Bulk Water (from Keller, 1966)

(Keller, 1966). Unfortunately, a mathematical model to account for the above effects has not been developed so far. If all these factors that affect the dc conductivity of water in pores of a rock are considered, then the dc conductivity might behave as shown in Figure 3 (see Keller, 1966). The linear relationship holds if there were no interaction between the water and the rock framework. The solid curve shows the more probable relation between rock resistivity and water resistivity when interaction between the water and the solid minerals takes place. At high salinities (high conductivity and low resistivity), the resistivity of the saline water in the pores is increased slightly by the greater viscosity of the water adsorbed on the grains. At lower salinities (lower conductivities and high resistivities) the resistivity of pore water approaches a maximum value rather than increasing indefinitely. This limit is determined by the amount of interaction. Both the increase in resistivity at high salinities and the decrease in resistivity at low salinities is more pronounced in fine-grained rocks than in coarse-grained rocks (Keller, 1966). For clay-rich rock, the limiting value may be as low as 0.1 ohm-m, while for coarse grained rock (e.g., concrete) with a low cation exchange capacity, this value may be as high as 10 ohm-m (Keller, 1966), which is the value shown in Figure 3.

The salinity of pore water in concrete bridges is usually much higher than 10 ppt (see computations in the chapter on 'numerical studies'). For this lower limit of $S_{sw} = 10$ ppt and $T = 20$ °C, one obtains an ionic conductivity of 1.5 mho/m which corresponds to a

resistivity of 0.67 ohm-n.. It can be seen from Figure 3 that this value is well within the "linear" range for a coarse-grained material. The pore water resistivity is only slightly higher in this range.

The above discussion holds good for the dc case. At higher frequencies, the deviation from linear relationship is further reduced because of the reduction in relaxation frequency for adsorbed water which tends to increase its dielectric conductivity (see Eqs. 5 and 13).

2.3 Models for Dielectric Properties of Concrete

This section presents three models which can be used to predict the dielectric properties of a mixture from the properties and volumetric proportions of the constituents. These models have been developed and verified for partially saturated rocks and will now be applied to concrete. The most significant constituents of concrete are coarse aggregate, fine aggregate, cement paste, air, water and salt. Reinforcing bars will not be considered here as a constituent, but their effect will be separately superimposed in the waveform synthesis model discussed later. It has already been mentioned in the previous section that only the chlorides which are actually present in solution form at any given time affects the dielectric properties of water and of the concrete mixture as a whole. The coarse aggregate as well as the fine aggregate in the mortar matrix have a relative dielectric constant in the range of 4.0 to 7.0 which is a typical value for common aggregates. The porosity of the coarse aggregate used in New England area (mainly granite) is usually very low (about 1%), hence it holds very little water. Thus, the aggregate's

dielectric constant has a very small imaginary part (loss factor) which may be ignored. The mortar matrix is very porous and the saline water in these pores is the primary constituent which contributes to the loss factor of the concrete mixture. Thus, concrete can be visualized as a three-phase mixture consisting of solid particles and air which have a real dielectric constant and saline water which has a complex dielectric permittivity. Three mixture models which are applicable to concrete are presented below.

(a) Complex Refractive Index Method (CRIM)

Refractive index (η_t) for a medium is defined as:

$$\eta_t = c_0 \sqrt{\mu_t \epsilon_0 \epsilon} \quad (26)$$

where,

c_0 = velocity of electromagnetic waves in vacuum =
 3×10^8 m/sec

μ_t = permeability of the medium = $\mu_0 = 4\pi \times 10^{-7}$ henry/m

for vacuum and most dielectric materials

ϵ = relative complex dielectric permittivity of the medium

ϵ_0 = dielectric permittivity of free space = 8.854×10^{-12}
farad/m.

The complex refractive index method (CRIM) asserts that the effective complex-refractive index for the mixture is given by the

volume average of the complex refractive indices of the constituents (Feng, 1985):

$$\sqrt{\epsilon} = (1-\phi) \sqrt{\epsilon_m} + (1-S)\phi \sqrt{\epsilon_a} + \phi S \sqrt{\epsilon_{sw}} \quad (27)$$

where,

ϕ = porosity of concrete = (volume of voids)/(total volume of concrete)

S = degree of saturation = (volume of water)/(volume of voids)

ϵ_m = relative dielectric permittivity of concrete solids $\cong 5.0$
(real)

ϵ_a = relative dielectric permittivity of air $\cong 1.0$ (real)

ϵ_{sw} = relative complex dielectric permittivity of water
(obtained using the model presented in the previous section)

ϵ = relative dielectric permittivity of resulting concrete mixture (a complex quantity)

The CRIM has been widely used for soils, rocks and concrete because of its simplicity, but has no theoretical basis. It gives reasonable results for $\epsilon''_{sw} \sim 1$ but gives highly inaccurate results for high salinity or low frequency; that is, when $\epsilon''_{sw} \gg 1$ (Feng, 1985). A comparison of the results predicted by this model and other more sophisticated models for the range of properties and frequencies encountered in concrete bridge decks has been carried out as a part of this research and is presented in Chapter 4 of this report.

Sometimes CRIM has been used as a real mixture law to predict the real part of ϵ by considering only the real part of dielectric permittivity of water (ϵ'_{sw}) and ignoring the imaginary part. The accuracy of such a simplification has also been discussed in the chapter on numerical studies (Chapter 4).

(b) Continuous Grain Size Distribution Model

This model assumes that the solid grains and air molecules in the concrete mixture are spherical in shape and have a continuous size distribution. The model has been derived by Feng and Sen (1985) based on the effective medium theory, which asserts that the effective complex relative dielectric constant of a mixture (ϵ) is given by (Feng, 1985):

$$\sum_i v_i \left(\frac{\epsilon - \epsilon_i}{2\epsilon + \epsilon_i} \right) = 0 \quad (28)$$

where ϵ_i denotes the dielectric permittivity of the individual constituents and v_i the corresponding volume fraction of the components. It has already been mentioned earlier that water is the only conducting phase in concrete, and the solid particles and air have a dielectric permittivity with a negligible imaginary part. The above effective medium theory is not directly applicable to concrete or rocks because it predicts that the dc conductivity becomes zero when the volume fraction ϕ_S of the conducting phase (water) drops below a critical value of 33% (Feng, 1985). For most rocks and

concrete, ϕS is almost always less than this critical value (Feng, 1985). This limitation of the effective medium theory can be removed by following a systematic procedure in which one starts with a background matrix of water in which small amounts of solid particles and air molecules are added in a number of steps. The smallest particles are added first and then followed by larger particles. Only the relative sizes of these particles need to be considered in the modelling. After each small addition the effective dielectric permittivity of the mixture is computed using Eq. (28), and the resulting mixture serves as a homogeneous background matrix for the next phase. The additions should be done in such a way that the final mixture has the constituents in the desired proportions. The amount of addition or inclusion of particles at any stage should be sufficiently less than 67% of the volume of the background matrix from the preceding stage. This removes the limitation of the equivalent media theory (Feng, 1985).

The model proposed by Feng and Sen (1985) assumes a continuous size distribution of the solid particles and air molecules, and considers infinitesimal inclusion of these particles at each step as described above. It can be shown from Eq. (28) that a change $d\epsilon$ in ϵ , the complex dielectric constant of the mixture at any stage, due to inclusions dv_m of solid grains and dv_a of air molecules is given by (Feng, 1985):

$$\frac{d\epsilon}{3\epsilon} = \frac{dv_m}{v_m + v_w + v_a} \cdot \frac{\epsilon_m - \epsilon}{\epsilon_m + 2\epsilon} + \frac{dv_a}{v_m + v_w + v_a} \cdot \frac{\epsilon_a - \epsilon}{\epsilon_a + 2\epsilon} \quad (29)$$

Here v_m , v_w and v_a denote the volume fraction of solid particles, water and air in the mixture.

In general, dv_m and dv_a can have arbitrary relation at each stage of the mixing process, but with the following constraint on the final ratio of the constituents:

$$v_a : v_m : v_w \text{ (final)} = (1-S) \phi : (1-\phi) : S \phi \quad (30)$$

Feng and Sen (1985) assume the following simple relationship between dv_m and dv_a at each step of the mixing process:

$$\frac{dv_a}{dv_m} = \frac{v_a}{v_m} \text{ (final)} = n' = \frac{(1-S)\phi}{(1-\phi)} \quad (31)$$

Thus, the medium has been built up by keeping the volume of water v_w fixed and adding infinitesimal amounts of solid grains and air molecules. The connectivity of water molecules is ensured at each step in this formulation even for unsaturated case, which is very crucial for predicting the dielectric conductivity. Substituting Eq. (31) into Eq. (29) and integrating the resulting equation with $v_a/v_m = n'$ held fixed and using the boundary condition in terms of the loss factor of the mixture as $\epsilon'' = \epsilon''_{sw}$ when $\phi S=1$ (with $S \rightarrow 1$ being taken first), one obtains an expression for the effective relative dielectric constant of the mixture ϵ as (Feng, 1985):

$$\phi S = \left(\frac{\epsilon_{sw}}{\epsilon} \right)^{1/3} \left(\frac{a'\epsilon^2 + b'\epsilon + c'}{a'\epsilon_{sw}^2 + b'\epsilon_{sw} + c'} \right)^{1/2} \quad (32)$$

$$\times \left[\frac{(2a'\epsilon + b' - \sqrt{b'^2 - 4a'c'}) (2a'\epsilon_{sw} + b' + \sqrt{b'^2 - 4a'c'})}{(2a'\epsilon + b' + \sqrt{b'^2 - 4a'c'}) (2a'\epsilon_{sw} + b' - \sqrt{b'^2 - 4a'c'})} \right]^{m'}$$

where,

$$n' = \phi (1-S)/(1-\phi)$$

$$a' = -2(1+n')$$

$$b' = 2 \epsilon_m - \epsilon_a + n' (2\epsilon_a - \epsilon_m)$$

$$c' = \epsilon_m \epsilon_a (1+n')$$

$$m' = -[(2\epsilon_m + \epsilon_a) + n'(2\epsilon_a + \epsilon_m)] / (2\sqrt{b'^2 - 4a'c'})$$

In the dc limit ($\omega \rightarrow 0$), Eq. (32) reduces to (Feng, 1985):

$$\sigma_0 = \sigma_i S^{n''} \phi^{m''}, \quad n'' = m'' = \frac{3}{2} \quad (33)$$

where σ_0 and σ_i refer to the dc conductivity of the mixture and water respectively.

Eq. (33) is nothing but the well known expression for Archie's Law (McNeill, 1980) which is commonly used to predict the dc conductivity for fully and partially saturated soils and rocks. A higher value of n'' and m'' (about 1.65 to 2.15) has been reported in the literature for fully saturated rocks (Keller, 1966). A value of 2.0 has been recommended by McNeil (1980) for partially saturated soil based on experimental results. It should be noted that Archie's law

is valid only in the dc limit whereas Eq. (32) predicts a frequency dependent behavior. The experimental data presented by Feng and Sen (1985) shows that Eq. (32) gives good results for rocks without flat shaped flaky grains, which is typical of claylike materials. The commonly used concrete aggregates do not contain such flaky grains in significant amount, and hence the assumption of spherical grain shape is a reasonable one.

(c) Discrete Grain Size Distribution Model

The previous model assumed a continuous size distribution of spherical grains. On the other hand, a model proposed by Madden and Williams (1989) using the equivalent media theory considers a discrete particle size distribution of spherical grains, which is thus a more realistic model for concrete. This model is also built in steps with the smallest particles being added first and followed by larger particles. As mentioned earlier, only the relative sizes of these particles need to be considered in the modelling. Grain size distribution is an important factor because it affects the internal structure of the given material, which in turn affects its dielectric properties. Water represents the smallest particle size and hence form the first background matrix, and an iterative procedure is followed to recompute the dielectric properties after each addition of a small amount of grains to this matrix. The connectivity of water molecules is ensured at each step even for unsaturated mixtures, just as in the previous model.

The proposed formulation deals with complex conductivities instead of complex dielectric constants, but these two concepts can easily be interchanged. Following the notation of Eqs. (3) to (7), the complex relative dielectric constant (ϵ) of a mixture can be written in terms of real and imaginary parts as:

$$\epsilon = \epsilon' + i\epsilon'' \quad (34a)$$

or

$$\epsilon = \epsilon' + \frac{i\sigma}{\omega\epsilon_0} \quad (34b)$$

Here σ denotes the dielectric conductivity of the medium defined as:

$$\sigma = \omega\epsilon''\epsilon_0 \quad (35a)$$

The complex conductivity (σ_c) is defined as:

$$\sigma_c = \sigma - i\epsilon'\epsilon_0\omega \quad (35b)$$

From Eqs. (34) and (35b), the relationship between ϵ and σ_c can be obtained as:

$$\sigma_c = -i\omega\epsilon\epsilon_0 \quad (36)$$

One can also formulate this model using the complex resistivity approach.

There are two basic approaches to the equivalent media calculations (Madden, 1989). One is the symmetric equivalent medium theory, which assumes all particles in the mixture to have spherical grain shape. The second approach, which is called the unsymmetric equivalent medium theory, arises from the important case where one of the components of the media is a matrix whose shape is essentially unknown. This is true with concrete mixture where the water phase forms the background matrix. The previously discussed continuous model and the discrete model to be discussed in this section both fall under the unsymmetric equivalent medium theory.

Madden and Williams (1989) have derived the following iterative mixture law for the above mentioned discrete case:

$$\sigma_n = \sigma_{n-1} - \sum_{j=1}^{k'} \frac{3(\sigma_{n-1} - \sigma_j)P_j \sigma_n}{(\sigma_j + 2\sigma_n)} \quad (37)$$

where,

- σ_n = complex conductivity of the mixture up to n^{th} step
- σ_{n-1} = complex conductivity of the mixture up to $(n-1)^{\text{th}}$ step
- σ_j = complex conductivity of j^{th} inclusion
- P_j = volume fraction of j^{th} inclusion
- k' = number of inclusions at each step.

Eq. (37) is a quadratic equation in σ_n which can be solved iteratively or using direct closed form solution at each step to obtain two roots

for σ_n . If there is only one inclusion at each step then $k'=1$. Among the two roots of Eq. (37), the root corresponding to the positive root of the discriminant is the one compatible with the sign convention used in Eq. (35).

The inclusions at each step substitute the grains in the background matrix up to the previous step, thus altering the proportion of these grains at each step. Thus the volume fractions (P_j) should be back-calculated in such a way that the matrix in the final step has all the constituents in the desired proportion. For the case of one inclusion at each step, the following recursive relation can be used to compute the volume fraction.

$$P_i = \frac{A_i}{(1-P_1)(1-P_2)\dots(1-P_{i-1})} \quad (38a)$$

$$P_1 = A_1 \quad (38b)$$

where,

P_i = volume fraction of the inclusion in i^{th} step

A_i = desired final proportion of the inclusion in i^{th} step

A_1 = final proportion for the largest size particle.

Among the three mixture models presented in this chapter, CRIM is the simplest one and has no theoretical foundation. The Continuous model and the Discrete model are more robust. Since concrete consists of discrete particle sizes, the Discrete model better

represents the physical reality. A comparison of the results predicted by the three mixture models will be presented in the next chapter.

CHAPTER 3

NUMERICAL STUDIES

3.1 Introduction

This chapter presents numerical results obtained using the models and equations discussed in the previous chapter. Firstly, the data used for this numerical study and its sources will be presented. The subsequent sections will describe the dielectric properties of concrete obtained by means of the various models. These results will then be examined and their implications will be discussed at the end of this chapter.

3.2 Data Used for Numerical Study

The various input parameters in these models for dielectric properties of concrete are temperature, frequency, porosity and degree of saturation in concrete, salinity of the pore water and dielectric properties of concrete solids. In case of the discrete grain size distribution model, a more detailed volumetric proportions of the concrete constituents is also required.

Temperatures of 20 °C and 5 °C have been considered in this study. The former represents conditions during fairly warm summer days while the latter is more typical of winter months. The radar antennas typically used for concrete bridge decks transmit energy in a narrow frequency band with half band-width spread of about 0.6

to 1.4 GHz and a central frequency of 1 GHz (Maser and Halabe, 1988). The porosity of newly cast concrete is usually of the order of 0.1 (Popovics, 1985) but disintegration due to freeze-thaw cycles can cause concrete in actual bridge decks to have a higher porosity of about 0.15, and even upto 0.2 in some extreme cases (Cady, 1983). For the purpose of this numerical study, porosities of 0.10 and 0.15 have been considered. The degree of saturation of the top and bottom one inch layer of concrete in conventional concrete bridge decks and the top one inch of stay-in-place (SIP) concrete decks (which are covered from bottom) varies between 40 or 50% in warm summer months to 75% in cold winter months (Carrier, 1975). The inner portion of the concrete usually retains a higher degree of saturation, fluctuating between 70% and 95% round the year (Carrier, 1975). This numerical study presents results for the entire range of 0 to 100%, but more emphasis has been placed on the 50% to 100% range.

No direct measurement of salinity of water present in the pores of concrete exposed to natural environment has been found in the literature. One exception to this is the case of concrete exposed to marine environment, which is not the area of application considered here. Hence, the salinity of pore water in concrete bridge decks has been indirectly ascertained based on field measurements of other related parameters. Values for free chloride and moisture content (expressed as percentage by weight of concrete) in core samples taken from deteriorated bridges in New England areas are presented in a report by Maser (1989). In two cases typical of older (> 25

years) decks, the free chloride content in top one-inch layer of concrete was found to be 0.25% and 0.34% (by weight of concrete) and the corresponding moisture content was 4.8% and 3.8% (by weight of concrete). To convert the percentage chloride content to NaCl equivalent, a multiplication factor equal to the ratio of molecular weight of NaCl ($= 23.0 + 35.5 = 58.5$) to the atomic weight of chlorine ($= 35.5$) has to be applied. This ratio turns out to be 1.65. Dividing the NaCl equivalent of the free chloride content by the corresponding moisture content, the salinity of pore water in the two cases is obtained as 86 and 148 parts per thousand by weight (ppt). A similar calculation on another deteriorated bridge deck showed a salinity of 132 ppt in the top one inch layer of concrete. The chloride content reduces significantly with depth in the concrete deck (Maser, 1989; Cady, 1983). Data presented by Cady and Weyers (1983) shows that the salinity is usually 21 ppt for new concrete decks. Such a small amount of salinity is inherent in concrete because of impurities in mixing water. Sometimes, salt is added to concrete during the mixing process to reduce the setting time. For the purpose of this numerical study, salinity values ranging between 12 and 90 ppt have been considered. This range represents the salinity of a typical deck during its first 20 years of service life.

The dielectric properties of saline water can be computed using the equations presented in Section 2.2. Now, the only remaining parameters are the dielectric constant for air, which is 1.0 and the dielectric constant for concrete solids, which is taken as 5.0. Typical values for granite, sandstones and limestones usually range between

4.0 and 7.0. The imaginary part of the complex dielectric permittivity is zero for air, and negligible for concrete solids compared to the value for saline water.

The discrete grain size distribution model requires more detailed volumetric proportions of the concrete constituents. The amount of water in the mix is given by ϕS , and the remaining void volume equal to $(1-S)\phi$ is filled with air. About two-thirds of this air volume is in the form of fine pores of size less than 100 nm and the remaining one-third constitutes coarse pores of approximate size 0.05 mm (Neville, 1983). The fine pores are the result of moisture evaporation during the setting process, while the coarse pores are entrained air generated during the mixing process. The entrained air helps in reducing freeze-thaw damage of exposed concrete (Neville, 1983). The fine aggregates (i.e., mortar paste of cement and sand) usually consists of particles with size less than 0.125 mm (Neville, 1983). The coarse aggregates (gravels) in a typical concrete mix usually have a size range of 1/2 to 3/2 inch (Neville, 1983) and a volumetric content of about 50%. The remaining half of the volume consists of fine aggregates and pores filled with air and water.

As mentioned earlier, the discrete grain size model is built in steps with the smallest particles being added first and followed by larger particles. At each step the volume fraction of the inclusion (P_i) should be significantly less than 67% of the total volume of background matrix. To take care of this constraint, the volume of particles in each category was further subdivided into small bins as follows:

- (a) volume fraction of water = $\phi S \equiv$ one bin (A₁₁)
- (b) volume fraction of air in fine pores = $\frac{2}{3} (1-S)\phi \equiv$ 3 bins (A₈, A₉, A₁₀)
- (c) volume fraction of fine aggregates = $(0.5 - \phi) \equiv$ 3 bins (A₅, A₆, A₇)
- (d) volume fraction of air in coarse pore = $\frac{1}{3} (1-S)\phi \equiv$ 1 bin (A₄)
- (e) volume fraction of coarse aggregates = $0.5 \equiv$ 3 bins (A₁, A₂, A₃)

The final volume fraction in the above bins have been chosen as follows:

$$A_{11} = \phi S$$

$$A_{10} = \frac{1}{9} (1 - S)\phi$$

$$A_9 = \frac{2}{9} (1-S)\phi$$

$$A_8 = \frac{1}{3} (1-S)\phi$$

$$A_7 = \frac{1}{5} (0.5 - \phi)$$

$$A_6 = \frac{3}{10} (0.5 - \phi)$$

$$A_5 = \frac{1}{2} (0.5 - \phi)$$

$$A_4 = \frac{1}{3} (1-S)\phi$$

$$A_3 = A_2 = A_1 = \frac{0.5}{3}$$

While building the mixture in this numerical model, the smallest size particle (i.e., A_{11}) is added first and the other particles A_{10} to A_1 are added sequentially with one bin at each step. It may be mentioned here that the final complex dielectric permittivity of the concrete mixture predicted by this model is not very sensitive to the assumptions made above regarding the volumetric content of the concrete constituents and the volume distribution in the bins, as long as all the P_i 's are significantly less than 0.67, as will be shown in the next section.

3.3 Numerical Results

This section presents the numerical results obtained using the models and equations presented in Chapters 2 and 3 and the data given in the previous section. The implications of these results are discussed in the following paragraph.

(a) Comparison of Complex CRIM vs Real CRIM Model

Table 1 shows the comparison of the results for real part of concrete dielectric permittivity predicted using CRIM (Eq. 27) and a simplified version of CRIM which has been termed here as "Real CRIM". The CRIM model in Eq. (27) uses the complex dielectric permittivity of saline water (ϵ_{sw}) and predicts complex permittivity

TABLE 1 COMPARISON OF COMPLEX CRIM vs REAL CRIM

$T = 20\text{ }^{\circ}\text{C}$, $f = 1\text{ GHz}$, $\phi = 0.1$,
 $\epsilon'(\text{air}) = 1.0$, $\epsilon'(\text{solids}) = 5.0$

| Degree of Saturation S | $S_{sw} = 12\text{ ppt. } \epsilon'_{sw} = 77.0$ | | $S_{sw} = 80\text{ ppt. } \epsilon'_{sw} = 57.4$ | |
|---------------------------------|--|--------------------------------|--|--------------------------------|
| | ϵ' Using CRIM | ϵ' Using Real CRIM | ϵ' Using CRIM | ϵ' Using Real CRIM |
| 0.0 | 4.5 | 4.5 | 4.5 | 4.5 |
| 0.2 | 5.2 | 5.1 | 5.4 | 5.0 |
| 0.4 | 5.9 | 5.9 | 6.3 | 5.6 |
| 0.6 | 6.7 | 6.7 | 7.2 | 6.3 |
| 0.8 | 7.6 | 7.5 | 8.2 | 7.0 |
| 1.0 | 8.5 | 8.4 | 9.2 | 7.7 |

(ϵ) for concrete. The Real CRIM model uses the real part of water permittivity (ϵ'_{sw}) and predicts the real part of concrete permittivity (ϵ'). This real version of CRIM is commonly used because of its simplicity. It can be seen from Table 1 that these two versions of CRIM model predict almost the same results for low salinity of water ($S_{sw} = 12.0$ ppt) but deviate to some extent for high salinity ($S_{sw} = 80.0$ ppt). The phase velocity and the reflection and transmission coefficients involve the square root of real dielectric permittivity ($\sqrt{\epsilon'}$), and the Real CRIM predicts a value lower by about 9% for $\sqrt{\epsilon'}$ in the high salinity and degree of saturation range, as can be seen from Table 1. Such a discrepancy is small in making velocity calculations, but can be significant in comparing reflection coefficients. Also, the Real CRIM model does not predict the loss factor which is related to attenuation.

(b) Comparison of the Three Mixture Models for Concrete

Table 2 presents the results predicted by the three complex mixture models for various values of porosity, salinity and degree of saturation at the 1 GHz frequency. The Discrete model could not predict any value for $S = 0.0$ because for this case the volume fraction of the inclusions (P_i) happen to exceed the critical value of 67% due to absence of water. It is possible to avoid this problem by changing the bin sizes for air when $S = 0.0$, which was not done here. It can be seen from this table that the real part of concrete dielectric permittivity predicted by the three models are very close (within 5% for $\sqrt{\epsilon'}$) for all cases. Field measurements on actual bridge decks

TABLE 2 COMPARISON OF THE THREE MIXTURE MODELS

(T = 20 °C, f = 1 GHz, ϵ' (air) = 1.0, ϵ' (solids) = 5.0)

(a) $\phi = 0.1$, $S_{sw} = 12$ ppt

| Degree of Saturation S | CRIM Model | | Continuous Model | | Discrete Model | |
|------------------------|-------------|---------------|------------------|---------------|----------------|---------------|
| | ϵ' | $k_I(m^{-1})$ | ϵ' | $k_I(m^{-1})$ | ϵ' | $k_I(m^{-1})$ |
| 0.0 | 4.5 | 0 | 4.5 | 0 | — | — |
| 0.2 | 5.2 | 0.9 | 5.2 | 1.0 | 5.2 | 0.9 |
| 0.4 | 5.9 | 1.7 | 6.0 | 2.0 | 5.9 | 1.6 |
| 0.6 | 6.7 | 2.6 | 6.8 | 3.0 | 6.6 | 2.3 |
| 0.8 | 7.6 | 3.4 | 7.6 | 4.0 | 7.3 | 3.0 |
| 1.0 | 8.5 | 4.3 | 8.5 | 5.0 | 7.9 | 3.7 |

TABLE 2 (continued)

(b) $\phi = 0.1, S_{sw} = 80$ ppt

| Degree of Saturation S | CRIM Model | | Continuous Model | | Discrete Model | |
|---------------------------------|---------------|---------------|---------------------|---------------|-------------------|---------------|
| | ϵ' | $k_I(m^{-1})$ | ϵ' | $k_I(m^{-1})$ | ϵ' | $k_I(m^{-1})$ |
| 0.0 | 4.5 | 0.0 | 4.5 | 0.0 | — | — |
| 0.2 | 5.4 | 3.5 | 5.3 | 4.4 | 5.4 | 3.4 |
| 0.4 | 6.3 | 7.1 | 6.1 | 8.9 | 6.2 | 6.3 |
| 0.6 | 7.2 | 10.6 | 6.9 | 13.0 | 6.9 | 9.3 |
| 0.8 | 8.2 | 14.1 | 7.6 | 18.0 | 7.6 | 12.4 |
| 1.0 | 9.2 | 17.6 | 8.4 | 23.0 | 8.3 | 15.7 |

TABLE 2 (continued)

(c) $\phi = 0.1$, $S_{sw} = 52$ ppt

| Degree of Saturation S | CRIM Model | | Continuous Model | | Discrete Model | |
|------------------------|-------------|---------------|------------------|---------------|----------------|---------------|
| | ϵ' | $k_I(m^{-1})$ | ϵ' | $k_I(m^{-1})$ | ϵ' | $k_I(m^{-1})$ |
| 0.5 | 6.5 | 6.8 | 6.4 | 8.3 | 6.4 | 6.0 |
| 0.6 | 7.0 | 8.1 | 6.8 | 9.9 | 6.8 | 7.1 |
| 0.7 | 7.4 | 9.5 | 7.2 | 12.0 | 7.1 | 8.3 |
| 0.8 | 7.9 | 10.8 | 7.6 | 13.0 | 7.5 | 9.4 |
| 0.9 | 8.4 | 12.2 | 8.0 | 15.0 | 7.8 | 10.6 |
| 1.0 | 8.8 | 13.5 | 8.4 | 17.0 | 8.1 | 11.9 |

TABLE 2 (Continued)

(d) $\phi = 0.15$, $S_{sw} = 52$ ppt

| Degree of Saturation S | CRIM Model | | Continuous Model | | Discrete Model | |
|---------------------------------|---------------|---------------|---------------------|---------------|-------------------|---------------|
| | ϵ' | $k_I(m^{-1})$ | ϵ' | $k_I(m^{-1})$ | ϵ' | $k_I(m^{-1})$ |
| 0.5 | 7.3 | 10.2 | 7.1 | 13.0 | 7.2 | 10.2 |
| 0.6 | 8.0 | 12.2 | 7.7 | 15.0 | 7.7 | 12.3 |
| 0.7 | 8.7 | 14.2 | 8.3 | 18.0 | 8.3 | 14.3 |
| 0.8 | 9.4 | 16.3 | 9.0 | 20.0 | 8.9 | 16.4 |
| 0.9 | 10.2 | 18.3 | 9.6 | 23.0 | 9.4 | 18.5 |
| 1.0 | 10.9 | 20.3 | 10.2 | 25.0 | 10.0 | 20.5 |

have indicated that dielectric permittivity is about 9.0 for deteriorated concrete, which suggests that the porosity should be around 0.15 (see Table 2d). There is a significant discrepancy in the value of attenuation coefficient (k_I) predicted by the three models. The discrepancy between the Discrete model and the CRIM model is about 13% for high salinity and degree of saturation with the CRIM Model predicting a higher attenuation. The Continuous model predicts an attenuation coefficient which is higher by even 25 to 40% compared to that predicted by the Discrete model for high values of salinity ($S_{sw} = 80.0$ ppt) and degree of saturation. Thus, it can be observed that the CRIM model is closer to the Discrete model than to the Continuous model.

The effect of the discrepancies in the attenuation coefficient predicted by the three models on the predicted waveforms can be understood from the following bridge deck calculations. Since the Continuous and Discrete models predict the highest and lowest values for attenuation coefficient (k_I), we will consider these two models here. For the purpose of this calculation, let us consider a 6 inch thick concrete deck with the top one inch layer having a salinity of 80 ppt and degree of saturation of 0.6, and the bottom five inches of concrete with a salinity of 12 ppt and degree of saturation of 0.8. From Table 2, the corresponding attenuation coefficients using the Continuous model are 13.0m^{-1} for top one inch layer and 4.0m^{-1} for the bottom five inch layer. The Discrete model predicts values for the attenuation coefficients of 9.3m^{-1} and 3.0m^{-1} , respectively. Since the transmitted wave has to travel twice the layer thickness

before it is received, the radar wave amplitude attenuates by a factor of $\exp(-2k_I x)$ as can be seen using Eq. (44). Hence, the attenuation factor of wave reflected from interface between the two concrete layers is obtained as 0.52 using the Continuous model and 0.62 using the Discrete model. The attenuation factor for the bottom reflection is a product of the attenuation factors in the top one inch and bottom five inches of concrete, and is obtained as 0.19 for Continuous model and 0.29 for Discrete model. Thus, the discrepancy in the two models ranges from 20% to 50%. If one includes all the reflection and transmission coefficient at the various interfaces (e.g., air-asphalt and asphalt-concrete boundary) then the discrepancy in the final synthesized waveform using the two models could be either higher or lower depending upon how close the properties of adjacent layers are. If one assumes that the attenuation coefficient (k_I) for the bottom five inches is also as high as that for the top one-inch layer (which could be the case for a severely deteriorated concrete deck), then the Continuous and Discrete models predict an attenuation factor for bottom reflection of 0.02 and 0.06, respectively.

These predicted attenuations are consistent with field observations. The field data from some deteriorated concrete bridge decks in New England area shows that under certain conditions it is difficult to see reflection from the bottom of the decks (Maser, 1989). The bottom reflections predicted here are more representative of field data than previous predictions (see Maser and Halabe, 1988). This was one of the motivations for this study (see Chapter 1).

However, the predictions from the two models (Discrete and Continuous) are significantly different. Of the three models, the Discrete model represents the closest representation of reality for reinforced concrete. The Continuous model would be more appropriate for materials with a continuous size distribution. The Continuous model appears to predict higher conductivity than the Discrete model. This can be understood physically, as discussed in the next paragraph. The CRIM model, which has no physical basis, predicts values somewhere in between those of the two physical models.

The above numerical results correspond to a frequency of 1 GHz. For low values of frequency (MHz range) or extremely high values of salinity the loss tangent for concrete ($\tan \delta = \epsilon''/\epsilon'$) is much greater than unity (see Eq. 46) and the CRIM model which has no theoretical basis, breaks down. On the other hand, the Continuous and Discrete models are valid even for $\tan \delta$ much larger than unity. Calculations carried out under this study (but not reported here) show that the dielectric conductivity of concrete (defined by Eq. 35a) is usually independent of frequency for frequencies below the MHz range. This value represents the dc conductivity of the medium, and can be obtained using the Archie's law expression for Continuous model with an exponent of 1.5 (see Eq. 33). Additional calculations have shown that a similar equation holds for the Discrete model as well, but with an exponent of about 1.7. The product ϕS in Eq. (33) always has a value less than unity. Thus, the Discrete model predicts lower values for dc and dielectric (high frequency) conductivity and

hence lower attenuation as compared to the Continuous model. This is due to the increased connectivity of water molecules when the grain size distribution is continuous. If the number of bins in the Discrete model is increased, then the results converge to the values predicted by the continuous model.

The discrepancy in the attenuation coefficient predicted by the three models must be considered in the context of the possible error in the estimation of salinity of the pore water in concrete. It has already been mentioned earlier that this salinity is indirectly estimated by dividing the free chloride content in the concrete (obtained from chloride content measurements in core samples) by the moisture content of the concrete (obtained from moisture content determination in the core sample). However, it is unknown whether the salinity of the water increases as the concrete loses its moisture or remains the same with change in degree of saturation. No research data is available on the amount of free chlorides actually remaining in dissolved state in concrete bridge decks. A numerical study was conducted as a part of this research using the mixture models described earlier in which the salinity of water was proportionately increased with reduction in degree of saturation, thus assuming that all the chlorides remained in dissolved state. For a degree of saturation of 0.7, this increased salinity corresponds to about 25% increase in the attenuation coefficient over the case for which the salinity is kept at the same level as that for 100% saturation, regardless of the model used. The change in salinity has a

very small effect on the real part of concrete permittivity (ϵ') which can also be seen from Table 2.

In the numerical study of the Discrete model, a particular size distribution has been assumed for the concrete constituents. A numerical study was conducted to determine the sensitivity of the predicted results to the size distribution. A modified concrete with a slightly different size distribution was assumed for this purpose. The modified concrete was assumed to have 65% coarse aggregates, with the remaining 35% of the volume occupied by fine aggregates, air pore and water, as opposed to the 50-50 ratio in case of the original concrete. In the original concrete, two-thirds of the total air volume was assumed to be in fine pores and one-third in coarse pores, but in the modified concrete, the total air volume was equally distributed among the coarse and fine pores. The porosity, water salinity and degree of saturation was kept at the same level for both cases. Table 3 shows the results predicted by the Discrete model for the original and modified concrete. As explained earlier, no values could be obtained for $S = 0.0$, because due to the absence of water, the volume fraction of subsequent inclusions (P_j) exceed the critical value of 0.67.

The results presented in Table 3 show the differences in dielectric properties between the original and modified concrete. The real part of dielectric permittivity (ϵ') is almost the same in the two cases, but the attenuation coefficient differ by as much as 8%. Thus, it can be concluded that the attenuation coefficient varies significantly with the size distribution.

TABLE 3 EFFECT OF SLIGHT CHANGE IN CONCRETE COMPOSITION ON RESULTS PREDICTED BY DISCRETE MODEL

T = 20 °C, f = 1 GHz, $\phi = 0.1$
 ϵ' (air) = 1.0, ϵ' (solids) = 5.0

| Degree of Saturation S | $S_{sw} = 12$ ppt | | | | $S_{sw} = 80$ ppt | | | |
|------------------------|--|---------------|---|---------------|--|---------------|---|---------------|
| | Discrete Model with Original Composition | | Discrete Model with Slightly Modified Composition | | Discrete Model with Original Composition | | Discrete Model with Slightly Modified Composition | |
| | ϵ' | $k_I(m^{-1})$ | ϵ' | $k_I(m^{-1})$ | ϵ' | $k_I(m^{-1})$ | ϵ' | $k_I(m^{-1})$ |
| 0.0 | — | — | — | — | — | — | — | — |
| 0.2 | 5.2 | 0.9 | 5.2 | 0.9 | 5.4 | 3.4 | 5.4 | 3.4 |
| 0.4 | 5.9 | 1.6 | 5.9 | 1.6 | 6.2 | 6.3 | 6.2 | 6.7 |
| 0.6 | 6.6 | 2.3 | 6.6 | 2.4 | 6.9 | 9.3 | 6.9 | 10.1 |
| 0.8 | 7.3 | 3.0 | 7.3 | 3.2 | 7.6 | 12.4 | 7.7 | 13.6 |
| 1.0 | 7.9 | 3.7 | 8.1 | 4.0 | 8.3 | 15.7 | 8.4 | 17.1 |

Since the Discrete model better represents the true concrete composition than the Continuous model, it should lead to better predictions for the electromagnetic properties of concrete. The theoretical models presented here are yet to be verified by means of either radar field data from actual bridge decks or small scale laboratory experiments.

(c) Study of Dielectric Properties of Concrete Using Discrete Model

This section investigates the typical behavior of concrete dielectric properties as a function of the various input parameters. It has already been mentioned earlier (see Table 2) that the salinity of pore water has a very small effect on the real part of concrete permittivity but has a large effect on the loss factor and attenuation coefficient. The frequency dependence of dielectric properties of concrete has been studied using the Discrete model, and the results are shown in Figures 4, 5, 6 and 7. Figure 4 shows that the real part of complex concrete permittivity (ϵ') is not very sensitive to frequency in the range of 0.6 to 3.0 GHz. Thus, the wave velocity (which is inversely proportional to $\sqrt{\epsilon'}$) is non-dispersive in this frequency range. Figures 5, 6 and 7 show the loss factor, attenuation coefficient and dielectric conductivity, and reveal a stronger dependence on frequency. The dispersive characteristic is stronger for higher degree of saturation, because water is the component which makes concrete a dispersive medium. It can also be seen that the attenuation coefficient and dielectric conductivity at high

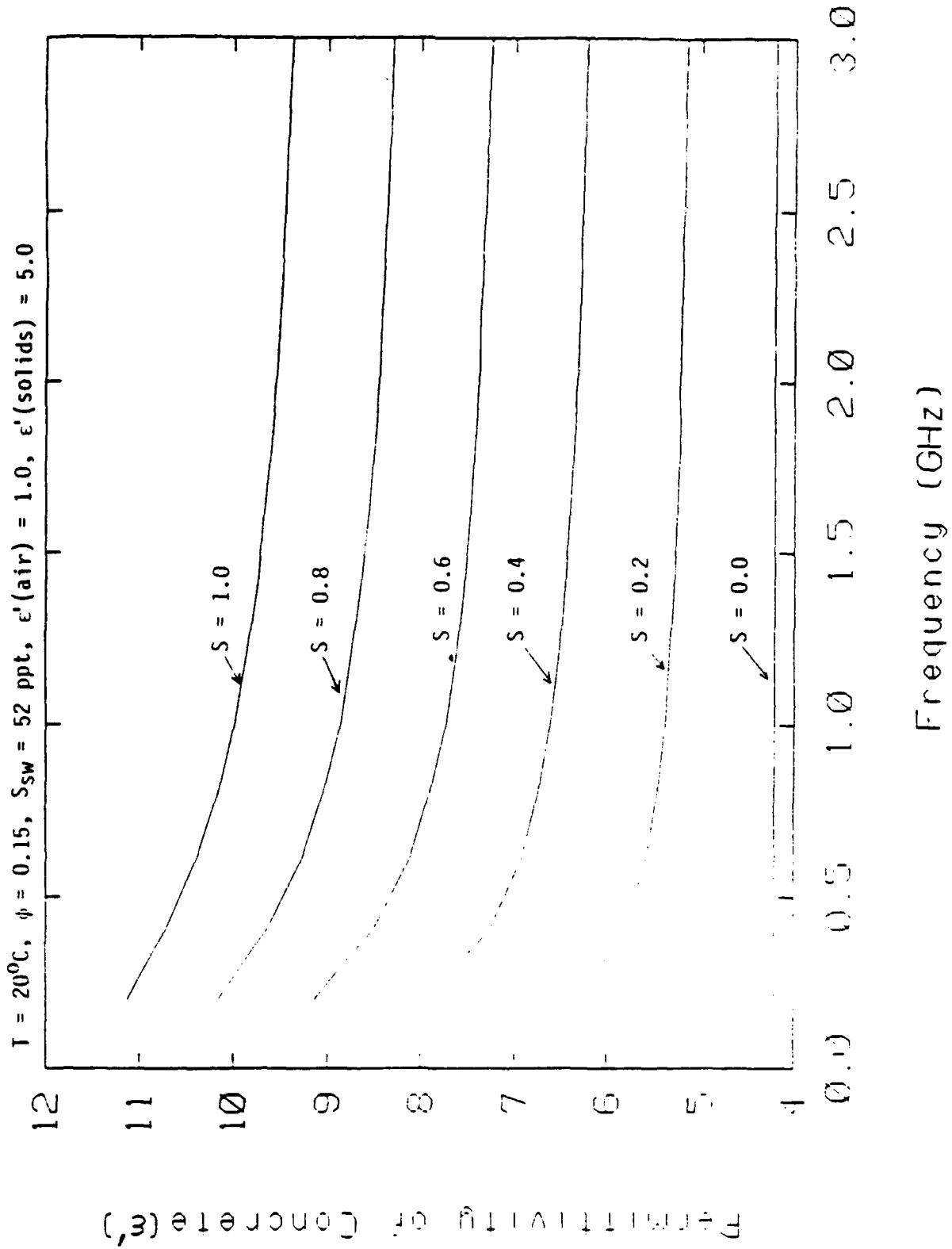
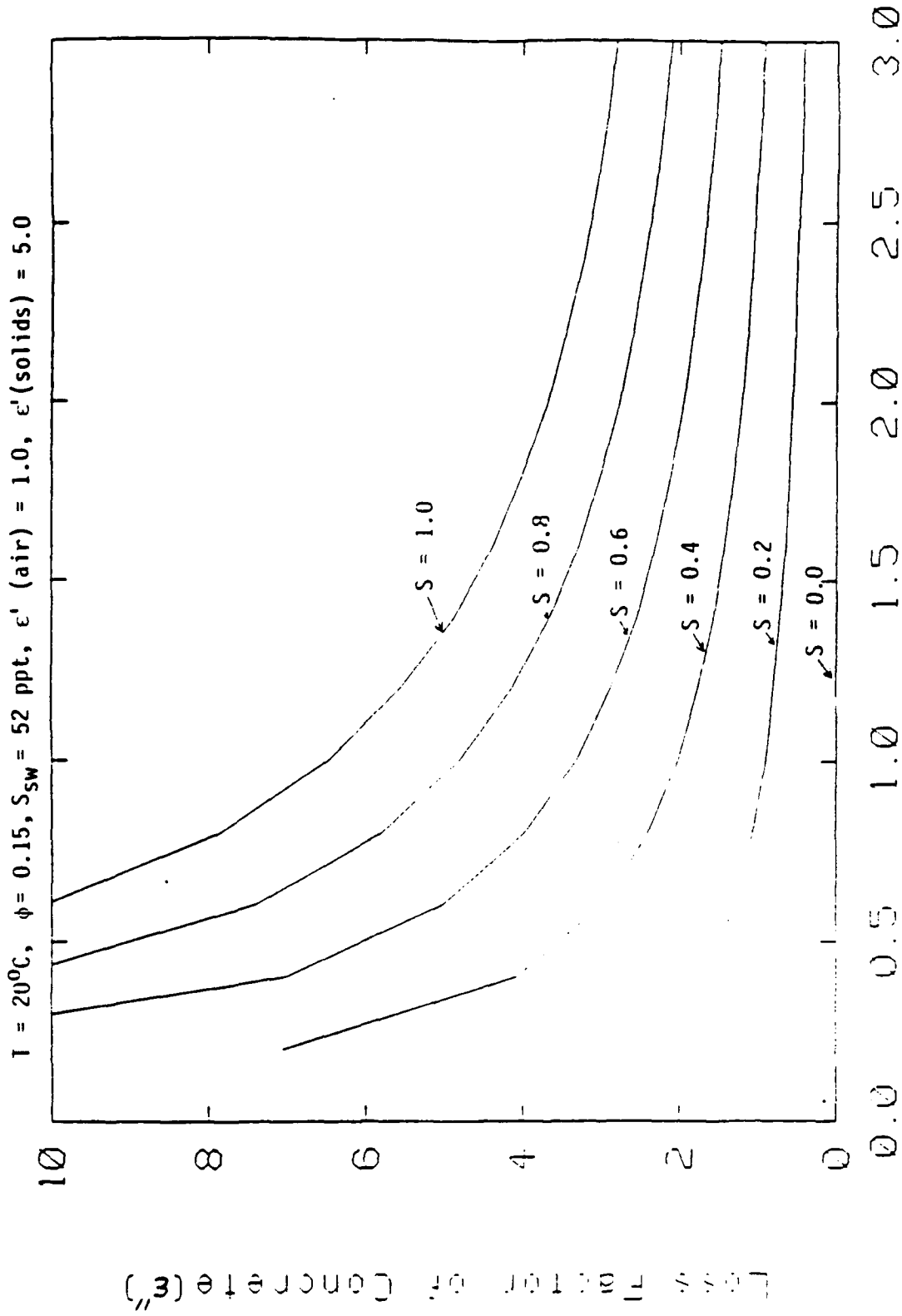
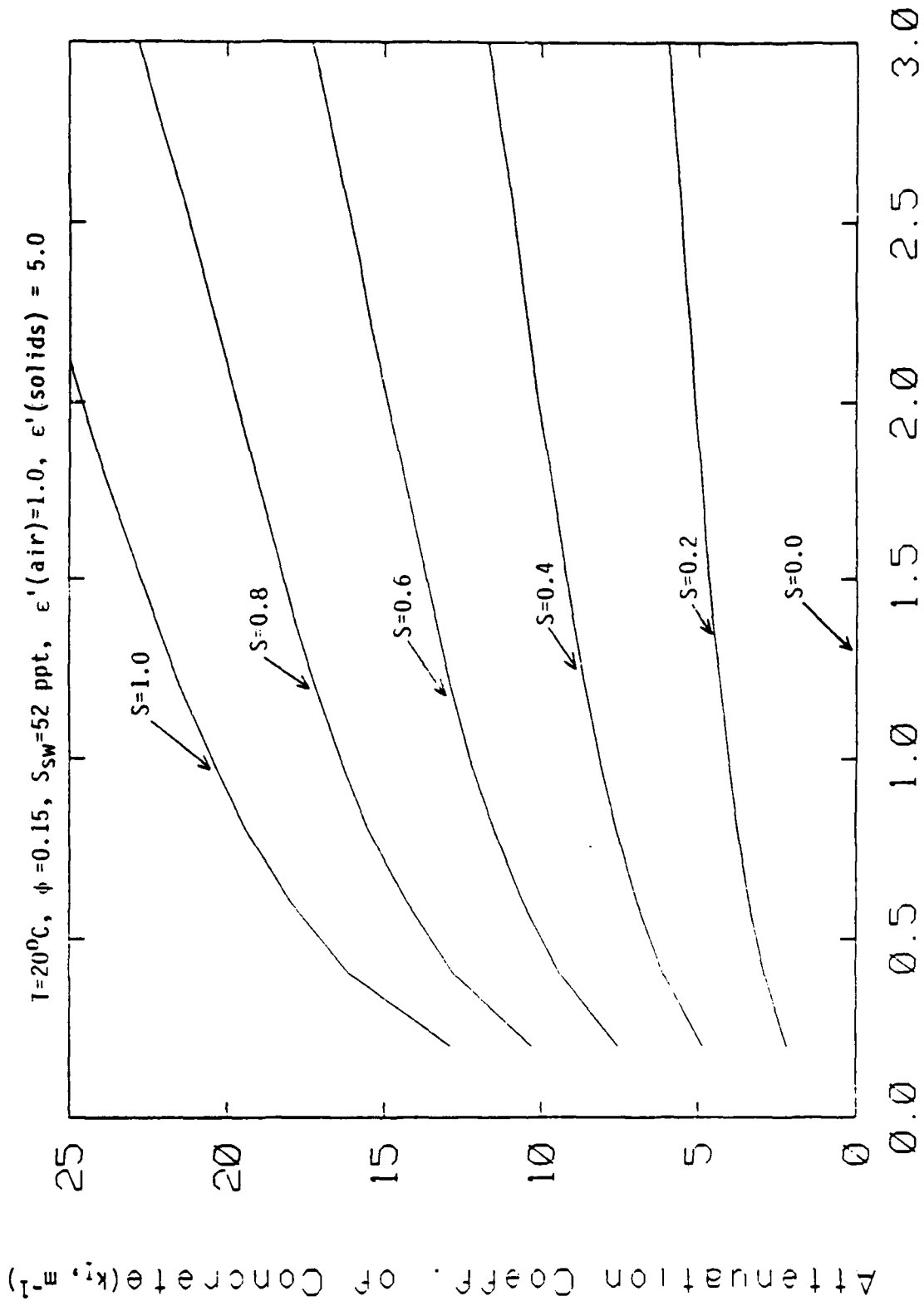


Figure 4. Permittivity of Concrete as a Function of Frequency (Discrete Model)



Frequency (GHz)

Figure 5. Loss Factor of Concrete as a Function of Frequency (Discrete Model)



Frequency (GHz)

Figure 6. Attenuation Coefficient of Concrete as a Function of Frequency (Discrete Model)

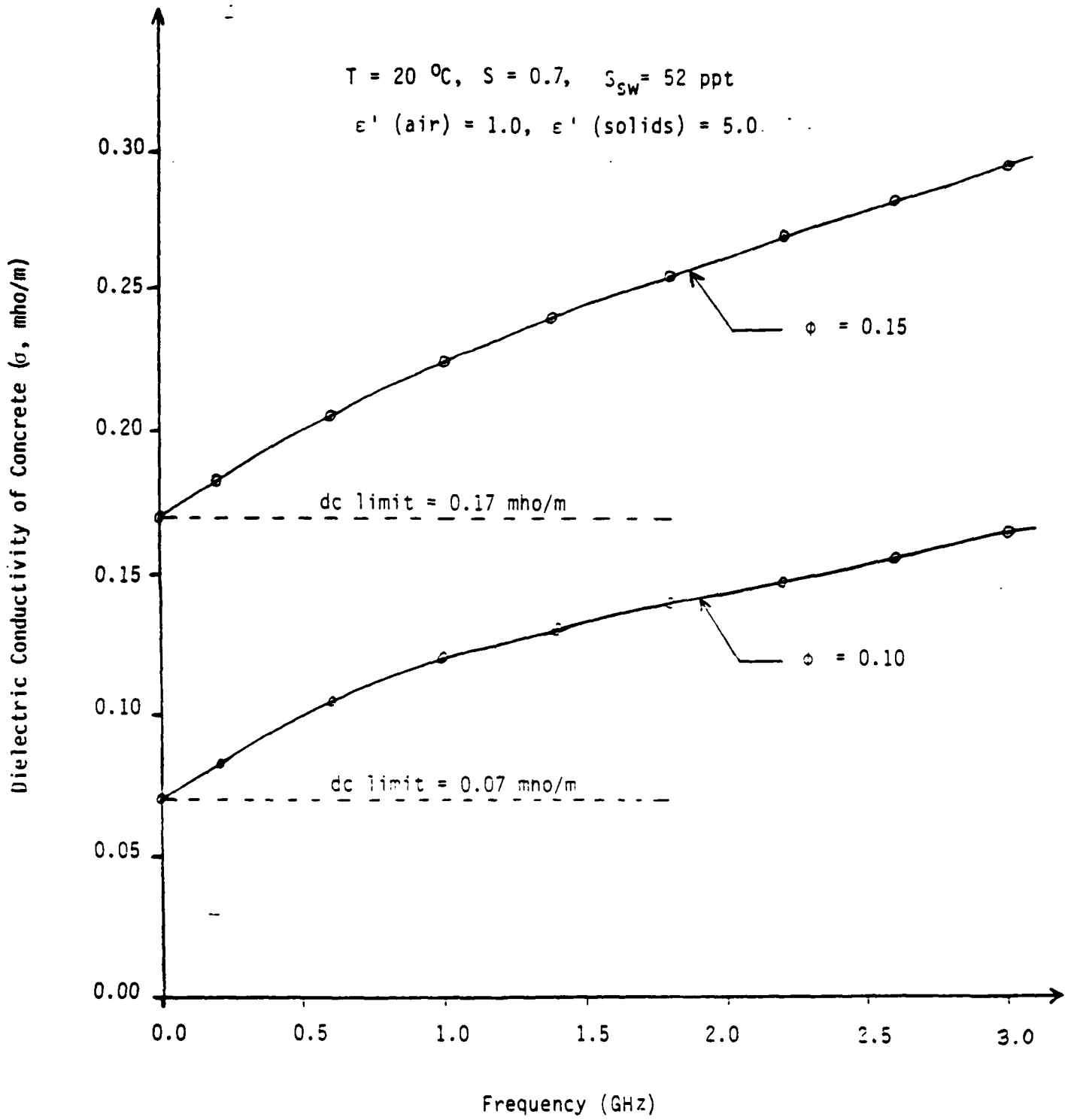


Figure 7. Dielectric Conductivity of Concrete (Discrete Model);

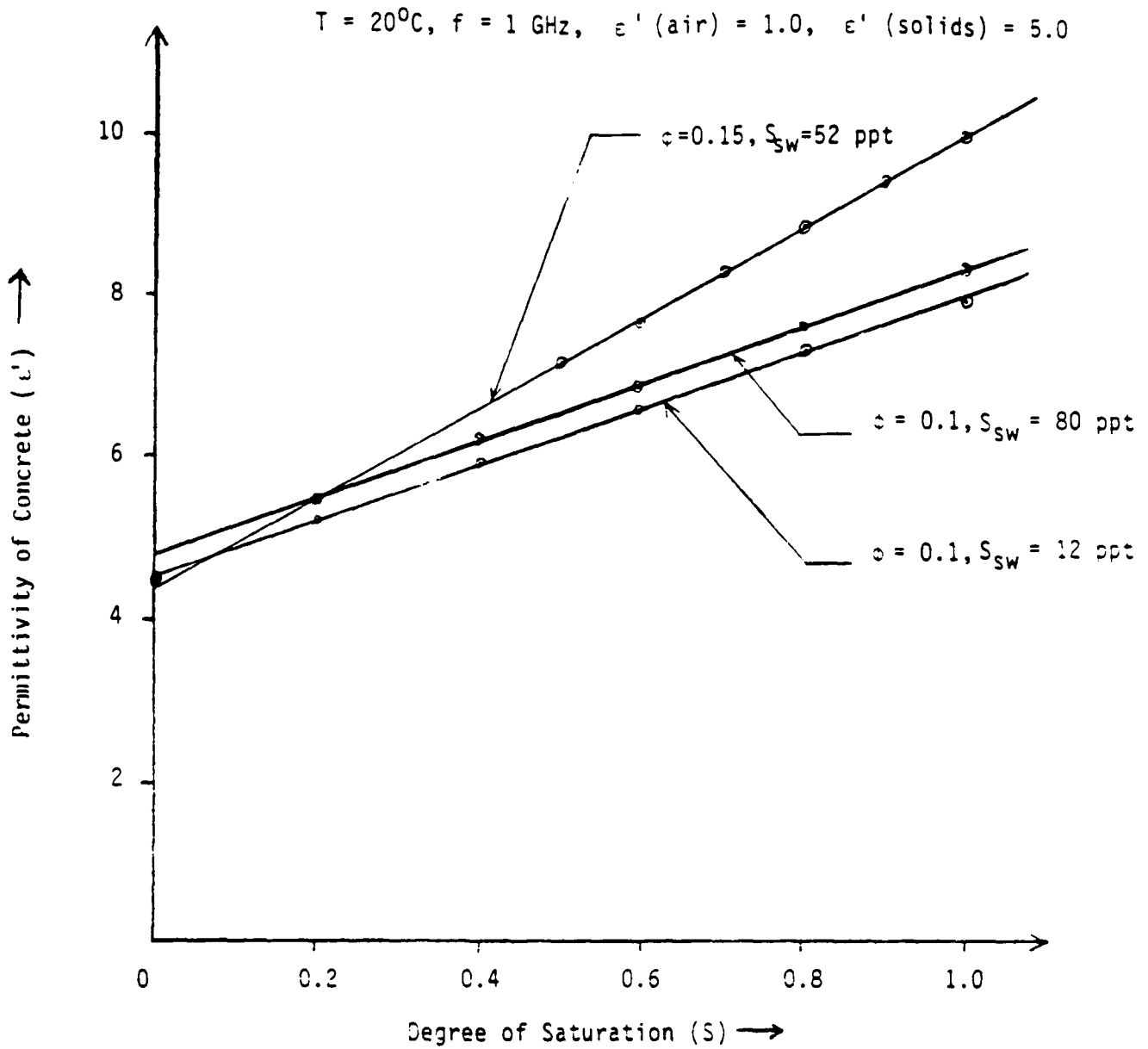


Figure 8. Permittivity of Concrete as a Function of Degree of Saturation (Discrete Model)

$T = 20^{\circ}\text{C}$, $f = 1 \text{ GHz}$, $\epsilon'(\text{air}) = 1.0$, $\epsilon'(\text{solids}) = 5.0$

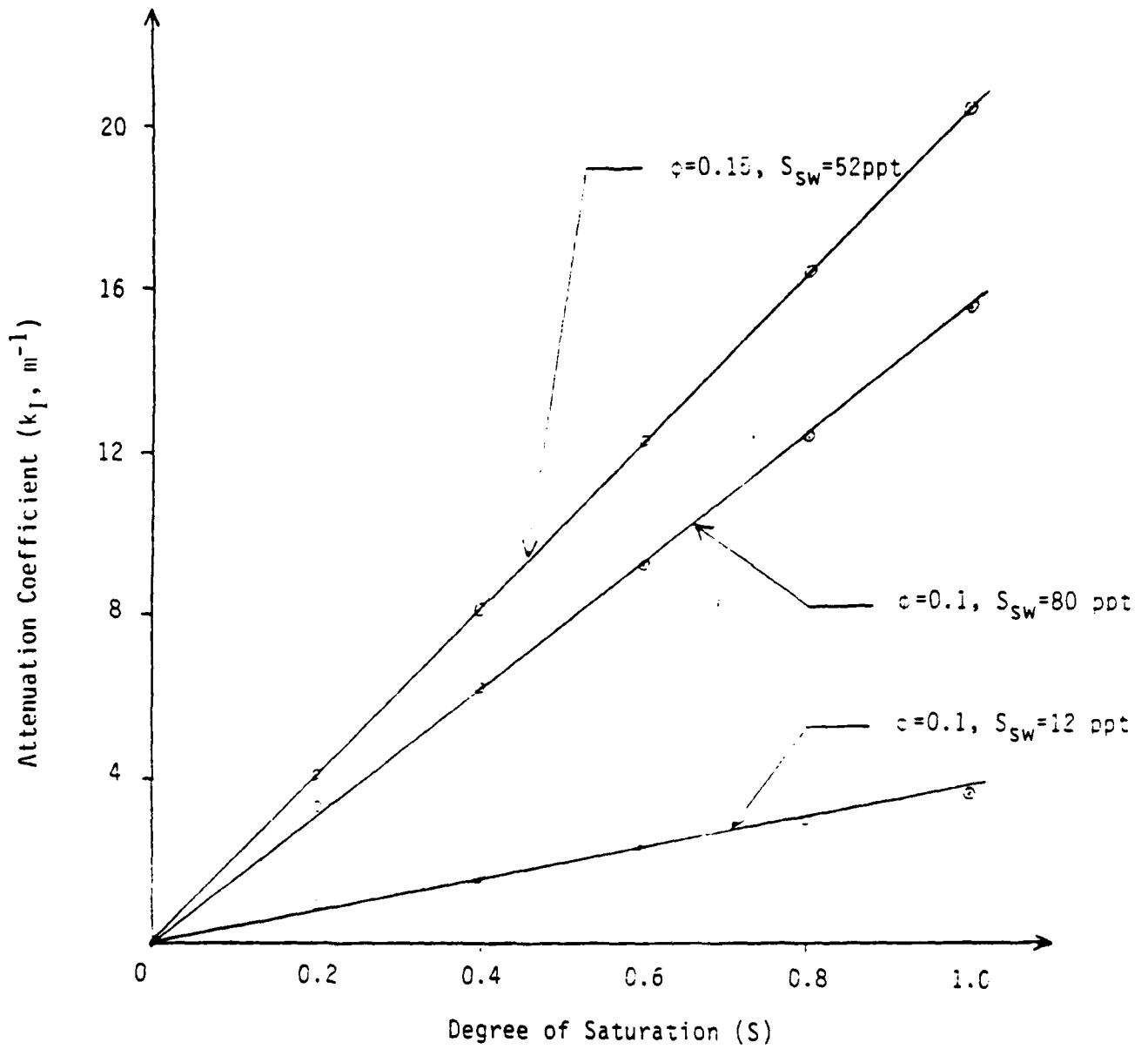


Figure 9. Attenuation Coefficient of Concrete as a Function of Degree of Saturation (Discrete Model)

frequency (near 1 GHz) is much higher than in the dc limit case. An interesting feature that can be noted from Figures 6 and 7 is that the frequency dependence of the attenuation coefficient and the dielectric conductivity is almost linear for frequencies above 0.6 GHz.

The discrete model used here can not compute results for $S=0$ due to numerical problems outlined earlier. Hence, the values corresponding to $S=0$ in Figures 4, 5, 6 and 7 have been computed using CRIM. Note that CRIM and Continuous model both predict the same results at $S=0$. Figures 8 and 9 correspond to data presented in Table 2, and show that the real part of concrete permittivity (ϵ') and the attenuation coefficient are linearly related to the degree of saturation. This suggests that the complex models presented in this research could be approximated by simpler equations for the prediction of concrete dielectric properties in the range of interest. This suggestion will be investigated in the next phase of this research.

All the above numerical study was conducted for a temperature of 20 °C. It has already been mentioned earlier (see Figures 1 and 2) that the dielectric properties of water have a significant temperature dependence. A numerical study was conducted to understand the effect of temperature on the dielectric properties of concrete and the results have been tabulated in Table 4. It can be seen that the temperature change has negligible effect on the real part of concrete dielectric permittivity (ϵ'). On the other hand, the attenuation coefficient reduces by about 25% when the temperature drops from 20 °C to 5 °C. This is because the water

**TABLE 4 EFFECT OF TEMPERATURE CHANGE ON
DIELECTRIC PROPERTIES OF CONCRETE**

$S_{sw} = 52.0$ ppt, $f = 1$ GHz, $\phi = 0.15$
 ϵ' (air) = 1.0, ϵ' (solids) = 5.0

| Degree of Saturation S | T = 20 °C | | T = 5 °C | |
|---------------------------------|-------------|---------------|-------------|---------------|
| | ϵ' | $k_I(m^{-1})$ | ϵ' | $k_I(m^{-1})$ |
| 0.0 | 4.2 | 0.0 | 4.2 | 0.0 |
| 0.2 | 5.4 | 4.1 | 5.3 | 3.2 |
| 0.4 | 6.6 | 8.2 | 6.5 | 6.3 |
| 0.6 | 7.7 | 12.3 | 7.6 | 9.3 |
| 0.8 | 8.9 | 16.4 | 8.8 | 12.4 |
| 1.0 | 10.0 | 20.5 | 10.0 | 15.5 |

dielectric conductivity drops significantly with temperature. Field data from some deteriorated bridge decks collected in warm summer days have indeed shown significantly higher attenuation compared to the data collected from the same bridge decks in cold winter days (Maser, 1989).

CHAPTER 4

CONCLUSIONS

The objective of this research was to characterize the velocity and attenuation of electromagnetic waves in reinforced concrete as a function of frequency, temperature, moisture content, chloride content and concrete mix constituents. This objective has been met by adaptation of theoretical models which have been developed and verified for partially saturated rocks. These models predict the electromagnetic properties of concrete by aggregating the electromagnetic properties of its most significant constituents which are water, salt, aggregates and air. Although the volume fraction of water in a concrete mixture is small, it has the most significant effect on concrete dielectric properties because of its high complex dielectric permittivity. The presence of salt in the water further influences the concrete dielectric properties.

Three models have been investigated in this study. One is a simple three-phase mixture law called CRIM which has no theoretical foundation. The other two models are more robust and have a theoretical basis. The Continuous grain size distribution model assumes that the solid grains and air molecules in the concrete mixture are spherical in shape and have a continuous size distribution. On the other hand, the Discrete grain size distribution

model considers a discrete particle size distribution of spherical grains, which is thus a more realistic model for concrete.

A comparison of the results predicted by the Discrete model with the complex CRIM model (Eq. 27) shows that the two models agree very well for real part of concrete dielectric permittivity (ϵ'). The attenuation coefficient predicted by the complex CRIM model is slightly higher (within 15%) compared to the Discrete model. The Continuous model predicts almost the same value for ϵ' but a significantly higher value for attenuation coefficient. This is due to the increased connectivity of water molecules when the grain size distribution is continuous.

Numerical studies have been carried out using the Discrete model. This model was chosen as the most accurate representation of real concrete. The results have shown that the salinity of pore water has a negligible effect on the real part of complex concrete permittivity but has a large effect on the loss factor and attenuation coefficient. The real part of complex concrete permittivity (ϵ') is not very sensitive to frequency in the range of 0.6 to 3.0 GHz. Thus, the wave velocity (which is inversely proportional to $\sqrt{\epsilon'}$) is non-dispersive in the high frequency range. However, the loss factor, attenuation coefficient and dielectric conductivity show a stronger dependence on frequency. The frequency dependence of attenuation coefficient and dielectric conductivity is almost linear for frequencies in the 0.6 to 3.0 GHz range. The real part of concrete permittivity and the attenuation coefficient also show a linear dependence with respect to the degree of saturation of the concrete mixture. This

suggests that the complex models presented in this study can be approximated in the range of interest by simple equations which can be used with a pocket calculator. Preliminary numerical studies have shown that even a real CRIM model (a simpler version of the complex CRIM) with proper modification of the exponent can approximate the other two complex models for the prediction of ϵ' within 5 to 10% in the high frequency range. The complex part of concrete permittivity (ϵ'') which is related to the dielectric conductivity (σ) can also be predicted within an error of 10% compared to the Discrete model by suitably modifying the exponents in the simple Archie's law (Eq. 33) or the complex CRIM (Eq. 27). Hence, future research should focus on developing these simpler equations to approximate the complicated models for the prediction of concrete dielectric properties in the high frequency range.

This study shows that the seasonal temperature variation usually encountered in field has negligible effect on the real part of concrete dielectric permittivity but has a significant impact on the attenuation coefficient of concrete, because the water dielectric conductivity drops significantly with temperature. A temperature drop from 20°C to 5°C causes a 25% reduction in the attenuation coefficient of concrete. Such a significant drop in attenuation has indeed been observed in bridge decks surveyed using radar in summer as well as in winter. Besides, the attenuations predicted with the new model are closer to the observed field data than the predictions made in previous studies which used the dc conductivity instead of dielectric conductivity.

The theoretical models presented in this study facilitate a rational prediction of dielectric properties of concrete based on the volumetric fraction and properties of its constituents. Future research should focus on the verification of these models by means of either radar field data from actual bridge decks or small scale laboratory experiments.

APPENDIX I

REFERENCES

- (1) Bell, J.R., Leonards, G.A., and Dolch, W.A., "Determination of Moisture Content of Hardened Concrete by its Dielectric Properties," Proceedings of the American Society for Testing and Materials, Vol. 63, 1963.
- (2) Cady, P.D., and Weyers, R.E., "Chloride Penetration and the Deterioration of Concrete Bridge Decks," Cement, Concrete, and Aggregates, ASTM, Vol. 5, No. 2, Winter 1983.
- (3) Carrier, R.E., Pu, D.C., and Cady, P.D., "Moisture Distribution in Concrete Bridge Decks and Pavements," SP 47-8, Durability of Concrete, American Concrete Institute Publications, 1975.
- (4) Dorsey, N.E., Properties of Ordinary Water Substance, Reinhold Publishing Corporation, New York, 1940.
- (5) Feng, S., and Sen, P.N., "Geometrical Model of Conductive and Dielectric Properties of Partially Saturated Rocks," Journal of Applied Physics, Vol. 58, No. 8, October, 1985.
- (6) Hoekstra, P., and Delaney, A., "Dielectric Properties of Soils at UHF and Microwave Frequencies," American Geophysical Union, 1974.
- (7) Keller, G.V., and Frischknecht, F.C., Electrical Methods in Geophysical Prospecting, Pergamon Press Inc., New York, 1966.
- (8) Klein, L.A., and Swift, C.T., "An Improved Model for the Dielectric Constant of Sea Water at Microwave Frequencies," IEEE Transactions on Antennas and Propagation, Vol. AP-25, No. 1, January 1977.
- (9) Kong, J.A., Electromagnetic Wave Theory, John Wiley and Sons, New York, 1986.
- (10) Madden, T.R., and Williams, E., "The Role of Size Distributions in Physical Properties of Inhomogeneous Materials," paper to be submitted to Journal of Geophysical Research in 1989.

- (11) Maser, K.R., "New Technology for Bridge Deck Assessment," New England Transportation Consortium Phase I Final Report, Center for Transportation Studies, MIT, February, 1989.
- (12) Maser, K.R., and Halabe, U.B., "Assessment of In-Situ Conditions Using Wave Propagation Techniques," US Army Research Office Final Technical Report, Center for Construction Research and Education, MIT, March, 1988
- (13) McNeill, J.D., Electrical Conductivity of Soils and Rocks, Technical Note TN-5, Geonics Ltd., October, 1980.
- (14) Neville, A.M., Properties of Concrete, Third Edition, The English Language Book Society (ELBS) and Pitman Publishing, Great Britain, 1983.
- (15) Popovics, S., "New Formulas for the Prediction of the Effect of Porosity on Concrete Strength," American Concrete Institute, No. 82-11, March-April, 1985.
- (16) Saxton, J., "Dielectric Dispersion in Pure Polar Liquids at Very High Radio-Frequencies, II, Relation of Experimental Results to Theory," Proceedings of Royal Society, 213A, 1952a.
- (17) Saxton, J.A., and Lane, J.A., "Electrical Properties of Sea Water," Wireless Engineer, October, 1952b.
- (18) Stogryn, A., "Equations for Calculating the Dielectric Constant of Saline Water," IEEE Transactions on Microwave Theory and Techniques, MIT-19, August, 1971.
- (19) Ulaby, F.T., Moore, R.K., and Fung, A.K., Microwave Remote Sensing, Vol. 3, Artech House Inc., MA, 1986.
- (20) Ulriksen, C.P.F., "Application of Impulse Radar to Civil Engineering," Doctoral thesis, Department of Engineering Geology, Lund University of Technology, Sweden, 1982.
- (21) Weast, R.C., ed., CRC Handbook of Chemistry and Physics, 67th edition, CRC Press Inc., Florida, 1986.

APPENDIX II

CONVERSION OF ELECTRICAL UNITS TO 'SI' UNITS

$$\text{coulomb} = \text{amp} \cdot \text{sec}$$

$$\text{volt} = \text{kg} \cdot \text{m}^2 \cdot \text{amp}^{-1} \cdot \text{sec}^{-3}$$

$$\text{farad} = \text{amp}^2 \cdot \text{sec}^4 \cdot \text{kg}^{-1} \cdot \text{m}^{-2}$$

$$\text{henry} = \text{kg} \cdot \text{m}^2 \cdot \text{amp}^{-2} \cdot \text{sec}^{-2}$$

$$\text{ohm} = \text{kg} \cdot \text{m}^2 \cdot \text{amp}^{-2} \cdot \text{sec}^{-3}$$

$$\text{S(Siemens)} = \text{mho} = \text{ohm}^{-1}$$

APPENDIX III

NUMERICAL PROCEDURE FOR OBTAINING ROOTS OF COMPLEX EQUATIONS

(a) Obtaining Real and Complex Roots

The complex mixture law equation (like the one in Eq. 32) involves the unknown complex quantity ϵ which has a real part ϵ' and an imaginary part ϵ'' which can be obtained using a complex root solver. A complex equation can also be written as two real equations as follows:

Real part of the expression = 0

Imaginary part of the expression = 0

Thus, a subroutine which finds roots (ϵ' and ϵ'') of a set of non-linear equations can also be employed. Most of the standard subroutines require good initial guesses for the solution to converge. Simple closed form equations like the CRIM model (see Eq. 27) can be used for obtaining such initial guesses for the roots. To be sure that the root has converged, it is advisable to use more than one root solver for the same equation.

(b) Computer Programs and Subroutines (FORTRAN-77)

The following computer programs (all with 'Double Precision') have been used:

- (i) M3•FOR and M4•FOR - Water conductivity, CRIM and Continuous Grain Size Models (the two programs use different complex root solvers)

- (ii) M5•FOR - Water Conductivity, CRIM and Discrete Grain Size Models

- (iii) PL1•FOR - Program for plotting curves

These programs are listed in the following pages. The root solving programs employ the IMSL subroutines ZSCNT and ZSPOW (see attached description) to solve for roots of a set of non-linear equations. Further documentation on IMSL library of subroutines is available in MIT's Micro VAX Computer Center (Room 1-249). The plotting programs use the 'Penplot' library subroutines which are also available in the above mentioned computer center.

```
C *****
C * PROGRAM NAME ----> M3.FOR----> NO SCREEN INPUT
C * SENDS ADDITIONAL OUTPUT IN 'M2.DAT' FOR PLOTTING
C * THIS PROGRAM INCORPORATES THEORETICAL MODELS FOR
C * (A) CONDUCTIVITY OF SALINE WATER
C * (B) DIELECTRIC PROPERTIES OF SALINE WATER
C * (C) MIXTURE LAWS FOR CONCRETE
C * INPUT IS READ FROM TERMINAL
C * OUTPUT IS SENT TO FILES CALLED 'M1.DAT' AND 'M2.DAT'
C * WHICH SHOULD BE OPENED BEFORE RUNNING THIS PROGRAM
C *****
C * THIS PROGRAM USES 'IMSL' SUBROUTINE 'ZSCNT' TO
C * EVALUATE COMPLEX ROOTS
C *****
C A,B = FUNCTIONS WHICH DEPEND ON 'SSW' AND 'T'
C C = FUNCTION OF 'ESW,EPW, F AND TSW'
C C1 = FUNCTION OF 'DEL' AND 'NSW'
C AA,BB,CC,DD = FUNCTIONS OF 'ETA, ESOL AND EAIR'
C ATT = ATTENUATION PARAMETER
C DEL = 25.0 - T
C E0 = DIELECTRIC PERMITTIVITY OF FREE SPACE
C EPSW = PARAMETER AT INFINITE FREQUENCY
C FOR BOTH PURE OR SALINE WATER
C EPW = PARAMETER FOR PURE WATER AT ZERO FREQUENCY
C EAIR = DIELECTRIC PERMITTIVITY OF AIR
C EPS = COMPLEX DIELECTRIC PERMITTIVITY FOR MIXTURE
C EPSI = IMAGINARY PART OF DIELECTRIC PERMITTIVITY FOR MIXTURE
C EPSR = REAL PART OF DIELECTRIC PERMITTIVITY FOR MIXTURE
C ESOL = DIELECTRIC PERMITTIVITY OF SOLID
C ESW = PARAMETER FOR SALINE WATER AT ZERO FREQUENCY
C ETA = FUNCTION OF 'P' AND 'S'
C EW = COMPLEX DIELECTRIC PERMITTIVITY FOR WATER
C EWI = IMAGINARY PART OF DIELECTRIC PERMITTIVITY FOR WATER
C EWI1,EWI2 = TWO COMPONENTS OF EWI
C EWR = REAL PART OF DIELECTRIC PERMITTIVITY FOR WATER
C F = FREQUENCY (GHz)
C F1,F2,F3,F4,F(1),F(2) = FUNCTIONS DEFINING COMPLEX
C EQUATION FOR THE SPHERICAL MODEL
C FCN = EXTERNAL FUNCTION FOR IMSL SUBROUTINE 'ZSCNT'
C FNORM = PARAMETER FOR IMSL SUBROUTINE 'ZSCNT'
C I = AN INTEGER NUMBER
C IER = PARAMETER FOR IMSL SUBROUTINE 'ZSCNT'
C IIM = IMAGINARY NUMBER = (0.0,1.0)
C ITMAX = PARAMETER FOR IMSL SUBROUTINE 'ZSCNT'
C J = AN INTEGER NUMBER
C K = COMPLEX WAVE NUMBER
C M1 = FUNCTION OF 'AA,BB,CC,EAIR AND ESOL'
C MU0 = PERMEABILITY OF FREE SPACE
C N = PARAMETER FOR IMSL SUBROUTINE 'ZSCNT'
C NSIG = PARAMETER FOR IMSL SUBROUTINE 'ZSCNT'
C NSW = NORMALITY OF SALINE WATER
C P = POROSITY OF MIXTURE
C PAR = PARAMETER FOR IMSL SUBROUTINE 'ZSCNT'
C PI = CONSTANT = 3.141592654
C S = DEGREE OF SATURATION
```

```

C      SI = FUNCTION WHICH DEPENDS ON 'SSW' AND 'T'
C      SIG25 = CONDUCTIVITY AT 25 C
C      SIGT = CONDUCTIVITY AT TEMPERATURE 'T'
C      SSW = SALT CONTENT OF WATER [gm/kg]
C      T = WATER TEMPERATURE
C      TPW = RELAXATION TIME FOR PURE WATER
C      TSW = RELAXATION TIME FOR SALINE WATER
C      W = ANGULAR FREQUENCY = 2.0*PI*F
C      WK = PARAMETER FOR IMSL SUBROUTINE 'ZSCNT'
C      X = PARAMETER FOR IMSL SUBROUTINE 'ZSCNT'
C      *****
C234567890
      INTEGER I,J,NSIG,N,ITMAX,IER
      REAL*8 A,B,C,C1,AA,BB,CC,DD,ATT,DEL
      REAL*8 EAIR,E0,EPSR,EPSI,EPW,EPW
      REAL*8 ESOL,ESW,ETA,EWI,EWI1,EWI2,EWR
      REAL*8 F,M1,MU0,NSW,P,PI,S,SI,SIG25,SIGT
      REAL*8 SSW,T,TPW,TSW,W
      REAL*8 PAR(2),X(2),FNORM,WK(42)
      COMPLEX*16 EW,EPS,IIM,K
      EXTERNAL FCN
      COMMON/U1/P,S,ESOL,EAIR,EW
      OPEN(UNIT=4,FILE='M1.DAT',STATUS='OLD')
      OPEN(UNIT=3,FILE='M2.DAT',STATUS='OLD')

C
      E0 = 8.854E-12
      PI = 3.141592654
      MU0 = PI*4.0E-7

C      READ INPUT PARAMETERS
C      *****
      S = 0.0
      DO 20 I=1,6
      F = 0.2
      DO 30 J=1,15
C      PRINT *, 'INPUT VALUE OF SSW(ppt),T(C) AND F(GHZ)'
C      READ(5,*) SSW,T,F
      SSW=80.0
      T=20.0
      F=F*1.0E9
C      PRINT *, 'INPUT VALUE OF P,S'
C      READ(5,*) P,S
      P=0.10

C
C      INPUT DATA
C      *****
      EAIR=1.0
      ESOL=5.0

C
C      COMPUTE WATER CONDUCTIVITY (MODEL FOR 'SSW' LESS
C      THAN 35.0 grams/liter)
C      *****
      DEL = 25.0 - T
      SI = 2.033E-2 + 1.266E-4*DEL + 2.464E-6*DEL*DEL
      SI = SI - SSW*(1.849E-5 - 2.551E-7*DEL + 2.551E-8*DEL*DEL)

```

- 71 -

```

SI = DEL*SI
SIG25 = 0.18252 - 1.4619E-3*SSW + 2.093E-5*SSW*SSW
SIG25 = SSW*(SIG25 - 1.282E-7*(SSW**3))
SIGT = SIG25*DEXP(-SI)

```

```

C
C COMPUTE REAL AND IMAGINARY PARTS OF DIELECTRIC
C PERMITTIVITY FOR SALINE WATER (MODEL FOR 'SSW'
C LESS THAN 35.0 grams/liter)
C *****

```

```

B = 1.0 + 2.282E-5*T*SSW - 7.638E-4*SSW
B = B - 7.760E-6*SSW*SSW + 1.105E-8*(SSW**3)
TPW = 1.1109E-10 - 3.824E-12*T + 6.938E-14*T*T
TPW = (TPW - 5.096E-16*(T**3))/(2.0*PI)
TSW = TPW*B

```

```

C
A = 1.0 + 1.613E-5*T*SSW - 3.656E-3*SSW
A = A + 3.21E-5*SSW*SSW - 4.232E-7*(SSW**3)
EPW = 87.134 - 1.949E-1*T - 1.276E-2*T*T
EPW = EPW + 2.491E-4*(T**3)
ESW = EPW*A

```

```

C
NSW = 1.707E-2 + 1.205E-5*SSW + 4.058E-9*SSW*SSW
NSW = NSW*SSW
IF(SSW.LE.35.0)GO TO 100

```

```

C
C COMPUTE WATER CONDUCTIVITY (MODEL FOR 'SSW'
C BETWEEN 35.0 AND 157.0 grams/liter)
C *****
C1 = 1.0 - 1.96E-2*DEL + 8.08E-5*DEL*DEL
C1 = C1 - NSW*DEL*(3.02E-5 + 3.92E-5*DEL)
C1 = C1 - NSW*NSW*DEL*(1.72E-5 - 6.58E-6*DEL)
SIG25 = 10.39 - 2.378*NSW + 0.683*NSW*NSW
SIG25 = SIG25 - 0.135*(NSW**3) + 1.01E-2*(NSW**4)
SIG25 = NSW*SIG25
SIGT = SIG25*C1

```

```

C
C COMPUTE REAL AND IMAGINARY PARTS OF DIELECTRIC
C PERMITTIVITY FOR SALINE WATER (MODEL FOR 'SSW'
C BETWEEN 35.0 AND 157.0 grams/liter)
C *****
B = 1.0 + 0.146E-2*T*NSW - 4.896E-2*NSW
B = B - 2.97E-2*NSW*NSW + 5.64E-3*(NSW**3)
TSW = TPW*B

```

```

C
A = 1.0 - 0.255*NSW + 5.15E-2*NSW*NSW - 6.89E-3*(NSW**3)
EPW = 88.045 - 0.4147*T + 6.295E-4*T*T + 1.075E-5*(T**3)
ESW = EPW*A

```

```

C
100 CONTINUE
EPSW = 4.9
W = 2.0*PI*F
C = (ESW-EPSW)/(1.0 + W*W*TSW*TSW)
EWR = EPSW + C
EWI1 = W*TSW*C
EWI2 = SIGT/(W*E0)

```

```

EWI = EW11 + EW12
IIM = (0.0,1.0)
EW = EWR + IIM*EWI
C
C COMPLEX-REFRACTIVE INDEX METHOD (CRIM)
C *****
EPS = P*S*CDSQRT(EW) + P*(1.0-S)*SQRT(EAIR)
EPS = EPS + (1.0-P)*SQRT(ESOL)
EPS = EPS*EPS
EPSR = DREAL(EPS)
EPSI = DIMAG(EPS)
C
C K = W*CDSQRT(EPS*MU0*E0)
ATT = DIMAG(K)
C
C OUTPUT OF NUMERICAL RESULTS
C *****
C CONDUCTIVITY MODEL
C -----
F = F/1.0E9
WRITE(4,18)
WRITE(4,10)
WRITE(4,11) SSW,NSW,T,F,SIGT,EWR,EW11,EW12,EWI
18 FORMAT(/4X,'CONDUCTIVITY MODEL')
10 FORMAT(4X,'SSW',5X,'NSW',5X,'T',5X,'F(GHZ)',4X,'SIGT',5X,'EWR',
&4X,'EW11',4X,'EW12',7X,'EWI')
11 FORMAT(7F8.2,2E11.3)
C
C CRIM MODEL
C -----
WRITE(4,19)
WRITE(4,12)
WRITE(4,13) EAIR,ESOL,P,S,EPSR,EPSI,ATT
19 FORMAT(/4X,'CRIM MODEL')
12 FORMAT(4X,'EAIR',4X,'ESOL',7X,'P',7X,'S',4X,'EPSR',
&4X,'EPSI',7X,'ATT')
13 FORMAT(6F8.2,E11.3)
C
C SPHERICAL GRAIN SHAPE MODEL
C *****
C INPUT PARAMETERS FOR SUBROUTINE 'ISCONT' WHICH
C SOLVES FOR COMPLEX ROOTS OF COMPLEX EQUATION
C -----
N = 2
NSIG = 3
ITMAX = 200
PAR(1) = 0.0
PAR(2) = 0.0
C
C INITIAL GUESS FOR ROOTS
C -----
X(1) = EPSR
X(2) = EPSI

```



```
C      F3 = 2.0*AA*EPS + BB - DD
      F4 = 2.0*AA*EPS + BB + DD
      F3 = F3 * (2.0*AA*EW + BB + DD)
      F4 = F4 * (2.0*AA*EW + BB - DD)
      F3 = (F3/F4)**M1

C      F1 = F1*F3
      F(1) = DREAL(F1) - S*P
      F(2) = DIMAG(F1)

C      RETURN
      END
```

```
C *****
C * PROGRAM NAME ----> M4.FOR----> NO SCREEN INPUT
C * SENDS ADDITIONAL OUTPUT IN 'M2.DAT' FOR PLOTTING
C * THIS PROGRAM INCORPORATES THEORETICAL MODELS FOR
C * (A) CONDUCTIVITY OF SALINE WATER
C * (B) DIELECTRIC PROPERTIES OF SALINE WATER
C * (C) MIXTURE LAWS FOR CONCRETE
C * INPUT IS READ FROM TERMINAL
C * OUTPUT IS SENT TO FILES CALLED 'M1.DAT' AND 'M2.DAT'
C * WHICH SHOULD BE OPENED BEFORE RUNNING THIS PROGRAM
C *****
C * THIS PROGRAM USES 'IMSL' SUBROUTINE 'ZSPOW' TO
C * EVALUATE COMPLEX ROOTS
C *****
C A,B = FUNCTIONS WHICH DEPEND ON 'SSW' AND 'T'
C C = FUNCTION OF 'ESW, EPSW, F AND TSW'
C C1 = FUNCTION OF 'DEL' AND 'NSW'
C AA, BB, CC, DD = FUNCTIONS OF 'ETA, ESOL AND EAIR'
C ATT = ATTENUATION PARAMETER
C DEL = 25.0 - T
C E0 = DIELECTRIC PERMITTIVITY OF FREE SPACE
C EPSW = PARAMETER AT INFINITE FREQUENCY
C FOR BOTH PURE OR SALINE WATER
C EPW = PARAMETER FOR PURE WATER AT ZERO FREQUENCY
C EAIR = DIELECTRIC PERMITTIVITY OF AIR
C EPS = COMPLEX DIELECTRIC PERMITTIVITY FOR MIXTURE
C EPSI = IMAGINARY PART OF DIELECTRIC PERMITTIVITY FOR MIXTURE
C EPSR = REAL PART OF DIELECTRIC PERMITTIVITY FOR MIXTURE
C ESOL = DIELECTRIC PERMITTIVITY OF SOLID
C ESW = PARAMETER FOR SALINE WATER AT ZERO FREQUENCY
C ETA = FUNCTION OF 'P' AND 'S'
C EW = COMPLEX DIELECTRIC PERMITTIVITY FOR WATER
C EWI = IMAGINARY PART OF DIELECTRIC PERMITTIVITY FOR WATER
C EW11, EW12 = TWO COMPONENTS OF EWI
C EWR = REAL PART OF DIELECTRIC PERMITTIVITY FOR WATER
C F = FREQUENCY (GHz)
C F1, F2, F3, F4, F(1), F(2) = FUNCTIONS DEFINING COMPLEX
C EQUATION FOR THE SPHERICAL MODEL
C FCN = EXTERNAL FUNCTION FOR IMSL SUBROUTINE 'ZSPOW'
C FNORM = PARAMETER FOR IMSL SUBROUTINE 'ZSPOW'
C I = AN INTEGER NUMBER
C IER = PARAMETER FOR IMSL SUBROUTINE 'ZSPOW'
C IIM = IMAGINARY NUMBER = (0.0, 1.0)
C ITMAX = PARAMETER FOR IMSL SUBROUTINE 'ZSPOW'
C J = AN INTEGER NUMBER
C K = COMPLEX WAVE NUMBER
C M1 = FUNCTION OF 'AA, BB, CC, EAIR AND ESOL'
C MU0 = PERMEABILITY OF FREE SPACE
C N = PARAMETER FOR IMSL SUBROUTINE 'ZSPOW'
C NSIG = PARAMETER FOR IMSL SUBROUTINE 'ZSPOW'
C NSW = NORMALITY OF SALINE WATER
C P = POROSITY OF MIXTURE
C PAR = PARAMETER FOR IMSL SUBROUTINE 'ZSPOW'
C PI = CONSTANT = 3.141592654
C S = DEGREE OF SATURATION
```

```

C      SI = FUNCTION WHICH DEPENDS ON 'SSW' AND 'T'
C      SIG25 = CONDUCTIVITY AT 25 C
C      SIGT = CONDUCTIVITY AT TEMPERATURE 'T'
C      SSW = SALT CONTENT OF WATER [gm/kg]
C      T = WATER TEMPERATURE
C      TPW = RELAXATION TIME FOR PURE WATER
C      TSW = RELAXATION TIME FOR SALINE WATER
C      W = ANGULAR FREQUENCY = 2.0*PI*F
C      WK = PARAMETER FOR IMSL SUBROUTINE 'ZSPOW'
C      X = PARAMETER FOR IMSL SUBROUTINE 'ZSPOW'
C      *****
C234567890
      INTEGER I,J,NSIG,N,ITMAX,IER
      REAL*8 A,B,C,C1,AA,BB,CC,DD,ATT,DEL
      REAL*8 EAIR,E0,EPSR,EPSI,EPW,EPW
      REAL*8 ESOL,ESW,ETA,EWI,EWI1,EWI2,EWR
      REAL*8 F,M1,MJ0,NSW,P,PI,S,SI,SIG25,SIGT
      REAL*8 SSW,T,TPW,TSW,W
      REAL*8 PAR(2),X(2),FNORM,WK(21)
      COMPLEX*16 EW,EPS,IIM,K
      EXTERNAL FCN
      COMMON/U1/P,S,ESOL,EAIR,EW
      OPEN(UNIT=4,FILE='M1.DAT',STATUS='OLD')
      OPEN(UNIT=3,FILE='M2.DAT',STATUS='OLD')

C
      E0 = 8.854E-12
      PI = 3.141592654
      MU0 = PI*4.0E-7

C      READ INPUT PARAMETERS
C      *****
      S = 0.0
      DO 20 I=1,6
      F = 0.2
      DO 30 J=1,15
C      PRINT *, 'INPUT VALUE OF SSW(ppt),T(C) AND F(GHZ)'
C      READ(5,*) SSW,T,F
      SSW=12.0
      T=20.0
      F=F*1.0E9
C      PRINT *, 'INPUT VALUE OF P,S'
C      READ(5,*) P,S
      P=0.10

C
C      INPUT DATA
C      *****
      EAIR=1.0
      ESOL=5.0

C
C      COMPUTE WATER CONDUCTIVITY (MODEL FOR 'SSW' LESS
C      THAN 35.0 grams/liter)
C      *****
      DEL = 25.0 - T
      SI = 2.033E-2 + 1.266E-4*DEL + 2.464E-6*DEL*DEL
      SI = SI - SSW*(1.849E-5 - 2.551E-7*DEL + 2.551E-8*DEL*DEL)

```

SI = DEL*SI
 SIG25 = 0.18252 - 1.4619E-3*SSW + 2.093E-5*SSW*SSW
 SIG25 = SSW*(SIG25 - 1.282E-7*(SSW**3))
 SIGT = SIG25*DEXP(-SI)

C
 C COMPUTE REAL AND IMAGINARY PARTS OF DIELECTRIC
 C PERMITTIVITY FOR SALINE WATER (MODEL FOR 'SSW'
 C LESS THAN 35.0 grams/liter)
 C *****

B = 1.0 + 2.282E-5*T*SSW - 7.638E-4*SSW
 B = B - 7.760E-6*SSW*SSW + 1.105E-8*(SSW**3)
 TPW = 1.1109E-10 - 3.824E-12*T + 6.938E-14*T*T
 TPW = (TPW - 5.096E-16*(T**3))/(2.0*PI)
 TSW = TPW*B

C
 A = 1.0 + 1.613E-5*T*SSW - 3.656E-3*SSW
 A = A + 3.21E-5*SSW*SSW - 4.232E-7*(SSW**3)
 EPW = 87.134 - 1.949E-1*T - 1.276E-2*T*T
 EPW = EPW + 2.491E-4*(T**3)
 ESW = EPW*A

C
 NSW = 1.707E-2 + 1.205E-5*SSW + 4.058E-9*SSW*SSW
 NSW = NSW*SSW
 IF(SSW.LE.35.0)GO TO 100

C
 C COMPUTE WATER CONDUCTIVITY (MODEL FOR 'SSW'
 C BETWEEN 35.0 AND 157.0 grams/liter)
 C *****

C1 = 1.0 - 1.96E-2*DEL + 8.08E-5*DEL*DEL
 C1 = C1 - NSW*DEL*(3.02E-5 + 3.92E-5*DEL)
 C1 = C1 - NSW*NSW*DEL*(1.72E-5 - 6.58E-6*DEL)
 SIG25 = 10.39 - 2.378*NSW + 0.683*NSW*NSW
 SIG25 = SIG25 - 0.135*(NSW**3) + 1.01E-2*(NSW**4)
 SIG25 = NSW*SIG25
 SIGT = SIG25*C1

C
 C COMPUTE REAL AND IMAGINARY PARTS OF DIELECTRIC
 C PERMITTIVITY FOR SALINE WATER (MODEL FOR 'SSW'
 C BETWEEN 35.0 AND 157.0 grams/liter)
 C *****

B = 1.0 + 0.146E-2*T*NSW - 4.896E-2*NSW
 B = B - 2.97E-2*NSW*NSW + 5.64E-3*(NSW**3)
 TSW = TPW*B

C
 A = 1.0 - 0.255*NSW + 5.15E-2*NSW*NSW - 6.89E-3*(NSW**3)
 EPW = 88.045 - 0.4147*T + 6.295E-4*T*T + 1.075E-5*(T**3)
 ESW = EPW*A

C
 100 CONTINUE
 EPSW = 4.9
 W = 2.0*PI*F
 C = (ESW-EPSW)/(1.0 + W*W*TSW*TSW)
 EWR = EPSW + C
 EW11 = W*TSW*C
 EW12 = SIGT/(W*E0)

```

EWI = EW11 + EW12
IIM = (0.0,1.0)
EW = EWR + IIM*EWI

```

```

C
C
C

```

```

COMPLEX-REFRACTIVE INDEX METHOD (CRIM)

```

```

*****

```

```

EPS = P*S*CDSQRT(EW) + P*(1.0-S)*SQRT(EAIR)
EPS = EPS + (1.0-P)*SQRT(ESOL)
EPS = EPS*EPS
EPSR = DREAL(EPS)
EPSI = DIMAG(EPS)

```

```

C

```

```

K = W*CDSQRT(EPS*MU0*E0)
ATT = DIMAG(K)

```

```

C
C
C

```

```

OUTPUT OF NUMERICAL RESULTS

```

```

*****

```

```

C
C

```

```

CONDUCTIVITY MODEL

```

```

-----

```

```

F = F/1.0E9
WRITE(4,18)
WRITE(4,10)
WRITE(4,11) SSW,NSW,T,F,SIGT,EWR,EW11,EW12,EWI
18  FORMAT(/4X,'CONDUCTIVITY MODEL')
10  FORMAT(4X,'SSW',5X,'NSW',5X,'T',5X,'F(GHz)',4X,'SIGT',5X,'EWR',
&4X,'EW11',4X,'EW12',7X,'EWI')
11  FORMAT(7F8.2,2E11.3)

```

```

C
C
C

```

```

CRIM MODEL

```

```

-----

```

```

WRITE(4,19)
WRITE(4,12)
WRITE(4,13) EAIR,ESOL,P,S,EPSR,EPSI,ATT
19  FORMAT(/4X,'CRIM MODEL')
12  FORMAT(4X,'EAIR',4X,'ESOL',7X,'P',7X,'S',4X,'EPSR',
&4X,'EPSI',7X,'ATT')
13  FORMAT(6F8.2,E11.3)

```

```

C
C
C

```

```

SPHERICAL GRAIN SHAPE MODEL

```

```

*****

```

```

C
C
C

```

```

INPUT PARAMETERS FOR SUBROUTINE 'ISPOW' WHICH
SOLVES FOR COMPLEX ROOTS OF COMPLEX EQUATION

```

```

-----

```

```

N = 2
NSIG = 3
ITMAX = 200
PAR(1) = 0.0
PAR(2) = 0.0

```

```

C
C
C

```

```

INITIAL GUESS FOR ROOTS

```

```

-----

```

```

X(1) = EPSR
X(2) = EPSI

```



```
C
F3 = 2.0*AA*EPS + BB - DD
F4 = 2.0*AA*EPS + BB + DD
F3 = F3 * (2.0*AA*EW + BB + DD)
F4 = F4 * (2.0*AA*EW + BB - DD)
F3 = (F3/F4)**M1

C
F1 = F1*F3
F(1) = DREAL(F1) - S*P
F(2) = DIMAG(F1)

C
RETURN
END
```

```
C *****
C * PROGRAM NAME ----> M5.FOR----> DISCRETE GRAIN SIZES MODEL
C * SENDS ADDITIONAL OUTPUT IN 'M2.DAT' FOR PLOTTING
C * AND IN 'M3.DAT' FOR CHECKING THE NUMERICAL SOLUTION STEPS
C * THIS PROGRAM INCORPORATES THEORETICAL MODELS FOR
C * (A) CONDUCTIVITY OF SALINE WATER
C * (B) DIELECTRIC PROPERTIES OF SALINE WATER
C * (C) MIXTURE LAWS FOR CONCRETE
C * INPUT IS READ FROM TERMINAL
C * OUTPUT IS SENT TO FILES CALLED 'M1.DAT', 'M2.DAT' AND
C * 'M3.DAT' WHICH SHOULD BE OPENED BEFORE RUNNING THIS PROGRAM
C *****
C A,B = FUNCTIONS WHICH DEPEND ON 'SSW' AND 'T'
C AN(I) = FINAL PROPORTION OF EACH SIZE COMPONENT
C C = FUNCTION OF 'ESW, EPSW, F AND TSW'
C C1 = FUNCTION OF 'DEL' AND 'NSW'
C AA,BB,CC = FUNCTIONS OF 'PN(I)' AND 'SIGC(I)'
C ATT = ATTENUATION PARAMETER
C DEL = 25.0 - T
C E0 = DIELECTRIC PERMITTIVITY OF FREE SPACE
C EPSW = PARAMETER AT INFINITE FREQUENCY
C FOR BOTH PURE OR SALINE WATER
C EPW = PARAMETER FOR PURE WATER AT ZERO FREQUENCY
C EAIR = DIELECTRIC PERMITTIVITY OF AIR
C EPS = COMPLEX DIELECTRIC PERMITTIVITY FOR MIXTURE
C EPSCRM = SAME AS 'EPSR' FOR S < 0.01
C EPSI = IMAGINARY PART OF DIELECTRIC PERMITTIVITY FOR MIXTURE
C EPSR = REAL PART OF DIELECTRIC PERMITTIVITY FOR MIXTURE
C ESOL = DIELECTRIC PERMITTIVITY OF SOLID
C ESW = PARAMETER FOR SALINE WATER AT ZERO FREQUENCY
C EW = COMPLEX DIELECTRIC PERMITTIVITY FOR WATER
C EWI = IMAGINARY PART OF DIELECTRIC PERMITTIVITY FOR WATER
C EW11,EWI2 = TWO COMPONENTS OF EWI
C EWR = REAL PART OF DIELECTRIC PERMITTIVITY FOR WATER
C F = FREQUENCY (GHz)
C I,II = AN INTEGER NUMBER
C IIM = IMAGINARY NUMBER = (0.0,1.0)
C J,JJ,KK = AN INTEGER NUMBER
C K = COMPLEX WAVE NUMBER
C MU0 = PERMEABILITY OF FREE SPACE
C NSW = NORMALITY OF SALINE WATER
C P = POROSITY OF MIXTURE
C PN(I) = PROPORTION OF INCLUSION AT EACH STEP
C PI = CONSTANT = 3.141592654
C S = DEGREE OF SATURATION
C SI = FUNCTION WHICH DEPENDS ON 'SSW' AND 'T'
C SIG25 = CONDUCTIVITY OF WATER AT 25 C
C SIGT = CONDUCTIVITY OF WATER AT TEMPERATURE 'T'
C SIGC(I) = CONDUCTIVITY OF INCLUSION AT EACH STEP
C SIGTC = COMPLEX CONDUCTIVITY OF THE MIXTURE
C SIGRC = REAL PART OF COMPLEX CONDUCTIVITY
C SIGIC = IMAGINARY PART OF COMPLEX CONDUCTIVITY
C SSW = SALT CONTENT OF WATER [gm/kg]
C T = WATER TEMPERATURE
C TPW = RELAXATION TIME FOR PURE WATER
```

```

C   TSW = RELAXATION TIME FOR SALINE WATER
C   W = ANGULAR FREQUENCY = 2.0*PI*F
C   *****
C234567890
      INTEGER I,J,II,JJ,KK
      REAL*8 A,B,C,C1,ATT,AN(11),DEL
      REAL*8 EAIR,E0,EPSCRM,EPSR,EPSI,EPW,EPW
      REAL*8 ESOL,ESW,EWI,EWI1,EWI2,EWR
      REAL*8 F,MU0,NSW,P,PI,PN(11),S,SI,SIG25
      REAL*8 SIGIC,SIGRC,SIGT,SSW,T,TPW,TSW,W
      COMPLEX*16 AA,BB,CC,EW,EPS,IIM,K
      COMPLEX*16 SIGC(11),SIGTC
      OPEN(UNIT=4,FILE='M1.DAT',STATUS='OLD')
      OPEN(UNIT=3,FILE='M2.DAT',STATUS='OLD')
      OPEN(UNIT=2,FILE='M3.DAT',STATUS='OLD')

C
      E0 = 8.854E-12
      PI = 3.141592654
      MU0 = PI*4.0E-7

C   READ INPUT PARAMETERS
C   *****
      S = 0.0
      DO 20 I=1,6
      F = 0.2
      DO 30 J=1,15
C     PRINT *, 'INPUT VALUE OF SSW(ppt),T(C) AND F(GHZ)'
C     READ(5,*) SSW,T,F
      SSW=52.0
      T=20.0
      F=F*1.0E9
C     PRINT *, 'INPUT VALUE OF P,S'
C     READ(5,*) P,S
      P=0.15

C
C   INPUT DATA
C   *****
      EAIR=1.0
      ESOL=5.0

C
C   COMPUTE WATER CONDUCTIVITY (MODEL FOR 'SSW' LESS
C   THAN 35.0 grams/liter)
C   *****
      DEL = 25.0 - T
      SI = 2.033E-2 + 1.266E-4*DEL + 2.464E-6*DEL*DEL
      SI = SI - SSW*(1.849E-5 - 2.551E-7*DEL + 2.551E-8*DEL*DEL)
      SI = DEL*SI
      SIG25 = 0.18252 - 1.4619E-3*SSW + 2.093E-5*SSW*SSW
      SIG25 = SSW*(SIG25 - 1.282E-7*(SSW**3))
      SIGT = SIG25*DEXP(-SI)

C
C   COMPUTE REAL AND IMAGINARY PARTS OF DIELECTRIC
C   PERMITTIVITY FOR SALINE WATER (MODEL FOR 'SSW'
C   LESS THAN 35.0 grams/liter)
C   *****

```

B = 1.0 + 2.282E-5*T*SSW - 7.638E-4*SSW
 B = B - 7.760E-6*SSW*SSW + 1.105E-8*(SSW**3)
 TPW = 1.1109E-10 - 3.824E-12*T + 6.938E-14*T*T
 TPW = (TPW - 5.096E-16*(T**3))/(2.0*PI)
 TSW = TPW*B

C

A = 1.0 + 1.613E-5*T*SSW - 3.656E-3*SSW
 A = A + 3.21E-5*SSW*SSW - 4.232E-7*(SSW**3)
 EPW = 87.134 - 1.949E-1*T - 1.276E-2*T*T
 EPW = EPW + 2.491E-4*(T**3)
 ESW = EPW*A

C

NSW = 1.707E-2 + 1.205E-5*SSW + 4.058E-9*SSW*SSW
 NSW = NSW*SSW
 IF(SSW.LE.35.0)GO TO 100

C

C

C

C

COMPUTE WATER CONDUCTIVITY (MODEL FOR 'SSW'
 BETWEEN 35.0 AND 157.0 grams/liter)

 C1 = 1.0 - 1.96E-2*DEL + 8.08E-5*DEL*DEL
 C1 = C1 - NSW*DEL*(3.02E-5 + 3.92E-5*DEL)
 C1 = C1 - NSW*NSW*DEL*(1.72E-5 - 6.58E-6*DEL)
 SIG25 = 10.39 - 2.378*NSW + 0.683*NSW*NSW
 SIG25 = SIG25 - 0.135*(NSW**3) + 1.01E-2*(NSW**4)
 SIG25 = NSW*SIG25
 SIGT = SIG25*C1

C

C

C

C

C

COMPUTE REAL AND IMAGINARY PARTS OF DIELECTRIC
 PERMITTIVITY FOR SALINE WATER (MODEL FOR 'SSW'
 BETWEEN 35.0 AND 157.0 grams/liter)

 B = 1.0 + 0.146E-2*T*NSW - 4.896E-2*NSW
 B = B - 2.97E-2*NSW*NSW + 5.64E-3*(NSW**3)
 TSW = TPW*B

C

A = 1.0 - 0.255*NSW + 5.15E-2*NSW*NSW - 6.89E-3*(NSW**3)
 EPW = 88.045 - 0.4147*T + 6.295E-4*T*T + 1.075E-5*(T**3)
 ESW = EPW*A

C

100

CONTINUE
 EPSW = 4.9
 W = 2.0*PI*F
 C = (ESW-EPSW)/(1.0 + W*W*TSW*TSW)
 EWR = EPSW + C
 EWI1 = W*TSW*C
 EWI2 = SIGT/(W*E0)
 EWI = EWI1 + EWI2
 IIM = (0.0,1.0)
 EW = EWR + IIM*EWI

C

C

C

COMPLEX-REFRACTIVE INDEX METHOD (CRIM)

 EPS = P*S*CDSQRT(EW) + P*(1.0-S)*SQRT(EAIR)
 EPS = EPS + (1.0-P)*SQRT(ESOL)
 EPS = EPS*EPS

```

EPSR = DREAL(EPS)
EPSI = DIMAG(EPS)
IF(S.LT.0.01)EPSCRM=EPSR
C
K = W*CDSQRT(EPS*MU0*E0)
ATT = DIMAG(K)
C
C
C OUTPUT OF NUMERICAL RESULTS
C *****
C
C CONDUCTIVITY MODEL
C -----
F = F/1.0E9
WRITE(4,18)
WRITE(4,10)
WRITE(4,11) SSW,NSW,T,F,SIGT,EWR,EWI1,EWI2,EWI
18 FORMAT(/4X,'CONDUCTIVITY MODEL')
10 FORMAT(4X,'SSW',5X,'NSW',5X,'T',5X,'F(GHz)',4X,'SIGT',5X,'EWR',
&4X,'EWI1',4X,'EWI2',7X,'EWI')
11 FORMAT(7F8.2,2E11.3)
C
C CRIM MODEL
C -----
WRITE(4,19)
WRITE(4,12)
WRITE(4,13) EAIR,ESOL,P,S,EPSR,EPSI,ATT
19 FORMAT(/4X,'CRIM MODEL')
12 FORMAT(4X,'EAIR',4X,'ESOL',7X,'P',7X,'S',4X,'EPSR',
&4X,'EPSI',7X,'ATT')
13 FORMAT(6F8.2,E11.3)
C
C DISCRETE GRAIN SIZE MODEL
C *****
C
C INPUT VALUES FOR FINAL MIX PROPORTIONS
C -----
AN(1) = 0.5/3.0
AN(2) = 0.5/3.0
AN(3) = 0.5/3.0
AN(4) = (1.0-S)*P/3.0
AN(5) = (0.5 - P)/2.0
AN(6) = 3.0*(0.5 - P)/10.0
AN(7) = 2.0*(0.5 - P)/10.0
AN(8) = (1.0-S)*P/3.0
AN(9) = 2.0*(1.0-S)*P/9.0
AN(10) = 2.0*(1.0-S)*P/18.0
AN(11) = P*S
C
C INPUT VALUES FOR COMPLEX DIELECTRIC
C PERMITTIVITY FOR EACH COMPONENT
C -----
SIGC(1) = 5.0
SIGC(2) = 5.0
SIGC(3) = 5.0
SIGC(4) = 1.0

```

```

SIGC(5) = 5.0
SIGC(6) = 5.0
SIGC(7) = 5.0
SIGC(8) = 1.0
SIGC(9) = 1.0
SIGC(10) = 1.0
SIGC(11) = EW

```

```

C
C CONVERT THE ABOVE VALUES TO
C COMPLEX CONDUCTIVITIES
C -----

```

```

DO 40 II=1,11
SIGC(II) = -IIM*W*E0*SIGC(II)
40 CONTINUE

```

```

C
C COMPUTE PN(I)
C -----
PN(1) = AN(1)
PN(2) = AN(2)/(1.0 - PN(1))
DO 50 II = 3,11
PN(II) = AN(II)
DO 50 JJ = 1,II-1
PN(II) = PN(II)/(1.0 - PN(JJ))
50 CONTINUE

```

```

C
C OUTPUT FOR CHECKING THE RESULTS
C -----

```

```

WRITE(2,21)
WRITE(2,22)(AN(II),II=1,11)
WRITE(2,23)
WRITE(2,22)(PN(II),II=1,11)
21 FORMAT(/4X,'(AN(I),I=1,11)')
22 FORMAT(6F10.4)
23 FORMAT(/4X,'(PN(I),I=1,11)')

```

```

C
C COMPUTE COMPLEX CONDUCTIVITY
C OF THE MIXTURE AT EACH STEP
C -----

```

```

SIGTC = SIGC(11)
DO 60 II=1,10
JJ = 11 - II
AA = 2.0
CC = -SIGTC*SIGC(JJ)
BB = 3.0*(SIGTC-SIGC(JJ))*PN(JJ)
BB = BB + SIGC(JJ) - 2.0*SIGTC
C
SIGTC = CDSORT(BB*BB - 4.0*AA*CC)
SIGTC = -(BB - SIGTC)/(2.0*AA)
IF(AN(11).LT.0.001.AND.JJ.EQ.10)SIGTC = SIGC(10)
SIGRC = DREAL(SIGTC)
SIGIC = DIMAG(SIGTC)

```

```

C
C OUTPUT FOR CHECKING THE ALGORITHM
C -----
WRITE(2,24)

```



```
C*****
C PROGRAM NAME--> PL1.FOR
C THIS PROGRAM PLOTS RESULTS OF DIELECTRIC DISPERSION CURVES FROM
C FILES M2.DAT. IT USES THE PENPLOT SUBROUTINE 'QPICTR'
C WHICH PASSES A SMOOTH CURVE THROUGH GIVEN POINTS. THIS PARTICULAR
C VERSION PLOTS DIELECTRIC PROPERTIES VS. FREQUENCY.
C BOTH X&Y AXES ARE IN NORMAL SCALES.
C*****
C
C23456789
C REAL F,EPSR,EPSI,ATT
C REAL XLO,YLO,XHI,YHI,DUMMY
C REAL XSCL(4),BALK(2,15)
C INTEGER I,J,K,IND(2),ISCL
C CHARACTER*50 XLAB,YLAB
C
C OPEN (UNIT=3,FILE='M2.DAT',STATUS='OLD')
C
C*****
C READ PARAMETER TO DETERMINE WHICH PLOT IS REQUIRED
C PRINT *, 'INPUT PLOT PARAMETER K & YLO & YHI'
C READ(5,*) K,YLO,YHI
C
C ENTER PARAMETERS FOR MINIMUM AND MAXIMUM LIMITS OF THE CURVE
C XLO=0.0
C XHI=3.0
C YLO=0.0
C YHI=10.0
C
C ENTER PARAMETERS FOR SMOOTH CURVE
C ISCL=-2
C XSCL(1)=XLO
C XSCL(2)=XHI
C XSCL(3)=YLO
C XSCL(4)=YHI
C
C LABELS
C XLAB='Frequency (GHz)'
C IF(K.EQ.1)YLAB='Permittivity of Concrete( )'
C IF(K.EQ.2)YLAB='Loss Factor of Concrete( )'
C IF(K.EQ.3)YLAB='Attenuation Coeff. of Concrete( )'
C
C
C READ DATA FROM INPUT FILES
C *****
C
C READ DATA FROM M2.DAT
C
C FIRST READ HEADER
C READ(3,30)DUMMY
C
C
C DO 50 I=1,6
C DO 40 J=1,15
C READ(3,30,END=45)F,EPSR,EPSI,ATT
```

```
30  FORMAT(3F8.2,E11.3)
    ATT=ABS(ATT)
    BALK(1,J)=F
    IF(K.EQ.1)BALK(2,J)=EPSR
    IF(K.EQ.2)BALK(2,J)=EPSI
    IF(K.EQ.3)BALK(2,J)=ATT
40  CONTINUE
45  IND(1)=15
    IND(2)=IND(1)

C
C  PLOT SMOOTH CURVES FOR THE GIVEN DATA
C  *****
C
    CALL QPICTR(BALK,2,IND(1),QY(2),QX(1),QXSCL(XSCL),
&QISCL(ISCL),QMOVE(C1),QLABEL(14),QXLAB(XLAB),QYLAB(YLAB))

C
50  CONTINUE
    STOP
    END
```

IMSL ROUTINE NAME - ZSCNT

PURPOSE - SOLVE A SYSTEM OF NONLINEAR EQUATIONS

USAGE - CALL ZSCNT (FCN, NSIG, N, ITMAX, PAR, X, FNORM, WK, IER)

ARGUMENTS

FCN - THE NAME OF A USER-SUPPLIED SUBROUTINE WHICH EVALUATES THE SYSTEM OF EQUATIONS TO BE SOLVED. FCN MUST BE DECLARED EXTERNAL IN THE CALLING PROGRAM AND MUST HAVE THE FOLLOWING FORM,

```
SUBROUTINE FCN(X,F,N,PAR)
DIMENSION X(N),F(N),PAR(1)
F(1)=
.
F(N)=
RETURN
END
```

GIVEN X(1)...X(N), FCN MUST EVALUATE THE FUNCTIONS F(1)...F(N) WHICH ARE TO BE MADE ZERO. X SHOULD NOT BE ALTERED BY FCN. THE PARAMETERS IN VECTOR PAR (SEE ARGUMENT PAR BELOW) MAY ALSO BE USED IN THE CALCULATION OF F(1)...F(N).

NSIG - THE NUMBER OF DIGITS OF ACCURACY DESIRED IN THE COMPUTED ROOT (INPUT).

N - THE NUMBER OF EQUATIONS TO BE SOLVED AND THE NUMBER OF UNKNOWNNS (INPUT).

ITMAX - THE MAXIMUM ALLOWABLE NUMBER OF ITERATIONS (INPUT).

PAR - PAR CONTAINS A PARAMETER SET WHICH IS PASSED TO THE USER SUPPLIED FUNCTION FCN. PAR MAY BE USED TO PASS ANY AUXILIARY PARAMETERS NECESSARY FOR COMPUTATION OF THE FUNCTION FCN. (INPUT)

X - A VECTOR OF LENGTH N. (INPUT/OUTPUT) ON INPUT, X IS THE INITIAL APPROXIMATION TO THE ROOT. ON OUTPUT, X IS THE BEST APPROXIMATION TO THE ROOT FOUND BY ZSCNT.

FNORM - ON OUTPUT, FNORM IS EQUAL TO $F(1)**2+...F(N)**2$ AT THE POINT X.

WK - WORK VECTOR OF LENGTH (N-1)*(3*N+8)

IER - ERROR PARAMETER. (OUTPUT)

TERMINAL ERROR

IER = 129 INDICATES THAT ZSCNT FAILED TO CONVERGE WITHIN ITMAX ITERATIONS. THE USER MAY INCREASE ITMAX OR TRY A NEW INITIAL GUESS.

IER = 130 INDICATES THE ALGORITHM WAS UNABLE TO IMPROVE ON THE RETURNED VALUE OF X. THIS SITUATION ARISES WHEN THE SOLUTION CANNOT BE DETERMINED TO NSIG DIGITS DUE TO ERRORS IN THE FUNCTION VALUES. IT MAY ALSO INDICATE THAT THE ROUTINE IS TRAPPED IN THE AREA OF A LOCAL MINIMUM. THE USER MAY TRY A NEW INITIAL GUESS.

- PRECISION/HARDWARE - SINGLE AND DOUBLE/H32
- SINGLE/H36,H48,H60
- REQD. IMSL ROUTINES - SINGLE/GGUBFS, LEQT2F, LUDATN, LUELMN, LUREFN,
UERSSET, UERTST, UGETIO, ZSCNU
- DOUBLE/GGUBFS, LEQT2F, LUDATN, LUELMN, LUREFN,
UERSSET, UERTST, UGETIO, VXADD, VXMUL, VXSTO,
ZSCNU
- NOTATION - INFORMATION ON SPECIAL NOTATION AND
CONVENTIONS IS AVAILABLE IN THE MANUAL
INTRODUCTION OR THROUGH IMSL ROUTINE UHELP

Algorithm

ZSCNT is based on an algorithm described in the reference cited below. At each step of the iterative process, there are $n+1$ trial solutions x^1, \dots, x^{n+1} . Multipliers, $a_j, j=1, 2, \dots, n+1$ are determined by solving the linear system:

$$\sum_{j=1}^{n+1} a_j = 1$$

$$\sum_{j=1}^{n+1} a_j f_i(x^j) = 0 \quad i=1, 2, \dots, n$$

Then the new trial solution is defined by

$$x = \sum_{j=1}^{n+1} a_j x_j .$$

See reference:

Wolfe, Phillip, "The Secant Method for Simultaneous Non-linear Equations", Communications of the ACM, Vol. 2, (1959).

Example

A 3 by 3 system of non-linear equations is to be solved. The values of the parameters in PAR are passed to FCN by the calling program.

Input:

INTEGER $n=3$, N, ITMAX, IER
REAL WK(68), X(3), PAR(3), FNORM
DATA PAR/27., 10., 7./
EXTERNAL FCN

```
N      = 3
NSIG   = 5
ITMAX  = 100
X(1)   = 4.
X(2)   = 4.
X(3)   = 4.
CALL ZSCNT (FCN,NSIG,N,ITMAX,PAR,X, FNORM,WK, IER
          .
          .
STOP
END
```

```
SUBROUTINE FCN(X,F,N,PAR)
REAL      X(3),F(3),PAR(3)
F(1)=X(1)+EXP(X(1)-1.)+(X(2)+X(3))**2-PAR(1)
F(2)=EXP(X(2)-2.)/X(1)+X(3)**2-PAR(2)
F(3)=X(3)+SIN(X(2)-2.)+X(2)**2-PAR(3)
RETURN
END
```

Output:

```
FNORM = .00000
X(1)  = 1.00001
X(2)  = 2.00000
X(3)  = 3.00000
```

IMSL ROUTINE NAME - ZSPOW

PURPOSE - SOLVE A SYSTEM OF NONLINEAR EQUATIONS

USAGE - CALL ZSPOW (FCN, NSIG, N, ITMAX, PAR, X, FNORM, WK, IER)

ARGUMENTS

FCN - THE NAME OF A USER-SUPPLIED SUBROUTINE WHICH EVALUATES THE SYSTEM OF EQUATIONS TO BE SOLVED. FCN MUST BE DECLARED EXTERNAL IN THE CALLING PROGRAM AND MUST HAVE THE FOLLOWING FORM,

```
      SUBROUTINE FCN(X,F,N,PAR)
      REAL X(N),F(N),PAR(1)
      F(1)=
      .
      F(N)=
      RETURN
      END
```

GIVEN X(1)...X(N), FCN MUST EVALUATE THE FUNCTIONS F(1)...F(N) WHICH ARE TO BE MADE ZERO. X SHOULD NOT BE ALTERED BY FCN. THE PARAMETERS IN VECTOR PAR (SEE ARGUMENT PAR BELOW) MAY ALSO BE USED IN THE CALCULATION OF F(1)...F(N).

NSIG - THE NUMBER OF DIGITS OF ACCURACY DESIRED IN THE COMPUTED ROOT. (INPUT)

N - THE NUMBER OF EQUATIONS TO BE SOLVED AND THE NUMBER OF UNKNOWN. (INPUT)

ITMAX - THE MAXIMUM ALLOWABLE NUMBER OF ITERATIONS. (INPUT) THE MAXIMUM NUMBER OF CALLS TO FCN IS ITMAX*(N+1). SUGGESTED VALUE = 200.

PAR - PAR CONTAINS A PARAMETER SET WHICH IS PASSED TO THE USER-SUPPLIED FUNCTION FCN. PAR MAY BE USED TO PASS ANY AUXILIARY PARAMETERS NECESSARY FOR COMPUTATION OF THE FUNCTION FCN. (INPUT)

X - A VECTOR OF LENGTH N. (INPUT/OUTPUT) ON INPUT, X IS THE INITIAL APPROXIMATION TO THE ROOT. ON OUTPUT, X IS THE BEST APPROXIMATION TO THE ROOT FOUND BY ZSPOW.

FNORM - ON OUTPUT, FNORM IS EQUAL TO $F(1)**2+...F(N)**2$ AT THE POINT X.

WK - WORK VECTOR OF LENGTH $N*(3*N-15)/2$

IER - ERROR PARAMETER. (OUTPUT)

TERMINAL ERROR

IER = 129 INDICATES THAT THE NUMBER OF CALLS TO FCN HAS EXCEEDED ITMAX*(N+1). THE USER MAY TRY A NEW INITIAL GUESS.

IER = 130 INDICATES THAT NSIG IS TOO LARGE. NO FURTHER IMPROVEMENT IN THE APPROXIMATE SOLUTION X IS POSSIBLE. THE USER SHOULD DECREASE NSIG.

IER = 131 INDICATES THAT THE ITERATION HAS NOT MADE GOOD PROGRESS. THE USER MAY TRY A NEW INITIAL GUESS.

- PRECISION/HARDWARE - SINGLE AND DOUBLE/H32
- SINGLE/H36,H48,H60
- REQD. IMSL ROUTINES - SINGLE/UERTST,UGETIO,VBLA=SNRM2,ZSPWA,
ZSPWB,ZSPWC,ZSPWD,ZSPWE,ZSPWF,ZSPWG
- DOUBLE/UERTST,UGETIO,VBLA=DNRM2,ZSPWA,
ZSPWB,ZSPWC,ZSPWD,ZSPWE,ZSPWF,ZSPWG
- NOTATION - INFORMATION ON SPECIAL NOTATION AND
CONVENTIONS IS AVAILABLE IN THE MANUAL
INTRODUCTION OR THROUGH IMSL ROUTINE UHELP

Algorithm

ZSPOW is based on the MINPACK subroutine HYBRD1, which uses a modification of M.J.D. Powell's hybrid algorithm. This algorithm is a variation of Newton's method which uses a finite difference approximation to the Jacobian and takes precautions to avoid large step sizes or increasing residuals.

See reference:

1. Moré, Jorge; Garbow, Burton; and Hillstom, Kenneth, User Guide for MINPACK-1, Argonne National Laboratory Report ANL-80-74, Argonne, Illinois, August, 1980.

Example

A 3 by 3 system of non-linear equations is to be solved.

Input:

```
INTEGER    N,NSIG,ITMAX,IER
REAL      PAR(3),X(3),FNORM,WK(36)
DATA     PAR/27.,10.,7./
EXTERNAL  FCN
N        = 3
NSIG     = 4
ITMAX    = 100
X(1)     = 4.0
X(2)     = 4.0
X(3)     = 4.0
CALL ZSPOW(FCN,NSIG,N,ITMAX,PAR,X,FNORM,WK,IER)
:
:
END
```

```
SUBROUTINE FCN (X,F,N,PAR)
INTEGER N
REAL X(N),F(N),PAR(1)
F(1)=X(1)+EXP(X(1)-1.0)+(X(2)+X(3))*(X(2)+X(3))-PAR(1)
F(2)=EXP(X(2)-2.0)/X(1)+X(3)*X(3)-PAR(2)
F(3)=X(3)+SIN(X(2)-2.0)+X(2)*X(2)-PAR(3)
RETURN
END
```

Output:

FNORM = .00000
X(1) = 1.00001
X(2) = 2.00000
X(3) = 3.00000